



Machine learning in concrete durability: challenges and pathways identified by RILEM TC 315-DCS towards enhanced predictive models

Woubishet Zewdu Taffese¹ · Benoît Hilloulin² · Yury Villagran Zaccardi³ · Afshin Marani⁴ · Moncef L. Nehdi⁵ · Muhammad Usman Hanif⁶ · Muralidhar Kamath⁷ · Sandra Nunes⁸ · Stefanie von Greve-Dierfeld⁹ · Antonios Kanellopoulos¹⁰

Received: 23 December 2024 / Accepted: 17 April 2025
© The Author(s) 2025

Abstract This review provides an in-depth examination of machine learning applications in assessing concrete durability from 2013 to 2024, with a particular focus on critical degradation mechanisms, including carbonation, chloride-induced deterioration, sulfate attack, frost damage, shrinkage, and corrosion. It underscores the field's heavy reliance on laboratory-based data and notes the limited use of field data and

the scarcity of newly generated datasets. The review reveals that most studies utilize existing literature-based datasets, with few contributing novel data and limited open access to these databases, which hampers broader validation and application. The review classifies the features analyzed in studies into categories such as mixture proportions, engineering properties, exposure conditions, test parameters, and chemical compositions, highlighting a growing emphasis on chemical compositions. Modeling approaches are predominantly standalone, though ensemble and hybrid models are increasingly prevalent, with ensemble models showing particularly strong performance in recent years. High accuracy is observed across studies, with ensemble models, neural networks, and hybrid models leading in performance. Furthermore, the review stresses the growing importance of model explainability, noting that model-agnostic methods like SHAP are frequently used and that the focus on explainability has increased. To propel the field forward, the review advocates for the development of diverse new datasets that include both the chemical and physical properties of various mix ingredients and improved data-sharing practices. It recommends adopting a multi-task learning approach to simultaneously address multiple deterioration mechanisms,

This review has been prepared by members of Focus Group 4 within RILEM TC 315-DCS “Data-driven concrete science” and further reviewed and approved by all members of the RILEM TC 315-DCS.

TC Membership

Chair: Sandra Nunes

Deputy Chair: Moncef Nehdi

TC Members: Sri Kalyana Rama Jyosyula; Reza Mohammadi-Firouz; Muhammad Usman Hanif; Neven Ukrainczyk; Yury Villagran-Zaccardi; Satoshi Fujimoto; Nivin Philip; Zhanzhao Li; Muralidhar Kamath; Ye Li; Volpatti Giovanni; Slawomir Czarnecki; Ling Wang; Afshin Marani; Benoît Hilloulin; Arnaud Delaplace; Antonios Kanellopoulos; Marcello Congro; Ravi Patel; Branko Šavija; Tulio Honorio de Faria; Gilberto Cidreira Kesterle; Bahman Ghiassi; Woubishet Zewdu Taffese; Jason Shun Fui Pei; Liberato Ferrara; Emilio Garcia-Taengua; Markus Greim; Ilhame Harbouz; Sandra Lucas; Lourdes Souza; Andrea Marcucci; Stefanie Von Greve-Dierfeld; Callum White; Rafael Abreu; Yihao Li; Kolawole Olonade; Zhang Zhe; Vitor Cunha; Ghezal Ahmad Jan Zia.

W. Z. Taffese (✉)

Department of Civil Engineering, Aalto University,
02150 Espoo, Finland
e-mail: woubishet.taffese@aalto.fi

B. Hilloulin

Nantes Université, Ecole Centrale Nantes, CNRS, GeM,
UMR 6183, 44000 Nantes, France



which can yield deeper insights and support the creation of more durable concrete structures.

Keywords Machine learning · Carbonation · Chloride attack · Frost damage · Shrinkage · Corrosion

Abbreviations

ACGRU	Attention-based convolutional gated recurrent unit
AdaBoost	Adaptive boosting
ALO	Ant lion optimization
ANN	Artificial neural network
BAS	Beetle antennae search
BO	Bayesian optimization
BPNN	Backpropagation neural network
BR	Bayesian ridge
CART	Classification and regression tree
CatBoost	Categorical boosting
CHAID	Chi-square automatic interaction detection
DNN	Deep neural network
DSC	Depth-wise separable convolution
DT	Decision tree
ELM	Extreme learning machine
FF	Feedforward
GA	Genetic algorithm
GAM	Generalized additive models
GB	Gradient boosting
GBM	Gradient boosting machines
GCV	Generalized cross-validation
GEP	Gene expression programming
GI	Garson index
GLM	Generalized linear models

GPR	Gaussian process regression
GRA	Grey relational analysis
GSA	Global sensitivity analysis
GWO	Grey wolf optimization
HGSO	Henry gas solubility optimization
ICA	Imperialist competitive algorithm
ICE	Individual conditional expectation
IV	Inverse variance
KDE	Kernel density estimation
KNN	K-nearest neighbors
NB	Naïve bayes
LightGBM	Light gradient-boosting machine
LR	Linear regression
MARS	Multivariate adaptive regression spline
MDI	Mean decrease impurity
MGGP	Multi-gene genetic programming
MLP	Multilayer perceptron
MLPNN	Multi-layer perceptron neural network
MLR	Multi-linear regression
MOEA/D	Multi-objective evolutionary algorithm based on decomposition
MPMR	Minimax probability machine regression
NSGA-II	Nondominated sorting genetic algorithm
OAT	One-at-a-time
PFI	Permutation feature importance
PSO	Particle swarm optimization
RBF	Radial basis function
RF	Random forest
RFE	Recursive feature elimination
RG	Ridge
RNN	Recurrent neural network
RReliefF	Regression relief feature selection

Y. Villagran Zaccardi
Materials and Chemistry Unit, Flemish Institute
for Technological Research (VITO), 2400 Mol, Belgium

A. Marani
Department of Civil and Mineral Engineering, University
of Toronto, Toronto M5S 1A4, Canada

M. L. Nehdi
College of Engineering and Physical Sciences, University
of Guelph, Guelph, ON, Canada

M. U. Hanif
Department of Technology and Innovation, SDU Civil
and Architectural Engineering, University of Southern
Denmark, Campusvej 55, 5230 Odense, Denmark

M. Kamath
NPD Division, Apple Chemie India Private Limited,
Nagpur, India

S. Nunes
Faculty of Civil Engineering and Geosciences, Delft
University of Technology, Delft, The Netherlands

S. von Greve-Dierfeld
TFB Technology and Research for Concrete Structures,
Wildeg, Switzerland

A. Kanellopoulos
Centre for Engineering Research, University
of Hertfordshire, Hatfield AL10 9AB, UK



RRHC	Random restart hill Climbing
SHAP	Shapley additive explanations
SOA	Seagull optimization algorithm
SOFM	Self-organizing feature map
SRC	Standardized regression coefficient
SSA	Sparrow search algorithm
SSIs	Sobol' sensitivity indices
SVM	Support vector machines
TBFI	Tree-based feature importance
TPE	Tree-structured parzen estimator
TWSVM	Twin support vector machines
VAF	Variation account factor
WNN	Wavelet neural network
WOA	Whale optimization algorithm
XGBoost	Extreme gradient boosting

1 Introduction

The durability of reinforced concrete (RC) infrastructure is of vital importance for the construction sector. Besides the strong correlation between durability and structural reliability, durability performance also affects long term maintenance costs as well as contributes to CO₂ emissions. In the United States alone, only for maintaining reinforced concrete decks due to poor durability the annual direct cost comes to a staggering \$2 billion [1]. Similar figures are being spent in Europe as well [2]. Assessing the durability of concrete is essential for ensuring the sustained performance and safety of infrastructure during its lifetime. Concrete, as the predominant construction material, undergoes various environmental stressors and loading conditions during its service life, leading to deterioration and potential structural concerns [3–5]. Hence, precise assessment techniques are imperative for detecting potential durability issues and implementing suitable remedial measures.

The assessment of concrete durability typically involves a series of standardized laboratory tests, including chloride permeability, water absorption, sulfate resistance, carbonation, freeze–thaw resistance, alkali-silica reaction, and abrasion tests, conducted in the early ages [6]. These tests employ diverse methodologies to evaluate essential durability aspects of concrete. Leveraging these laboratory tests in the early stages, engineers obtain valuable data to inform material selection, optimize mix designs, and implement construction practices conducive to

enhancing the durability and longevity of concrete structures.

However, conducting multiple tests to evaluate durability performance is resource-intensive and time-consuming. Hence, empirical models offer a pragmatic complement to reduce laboratory tests for assessing concrete durability. Derived from statistical analyses of experimental data, these models provide simplified methodologies for estimating concrete properties and behaviors without extensive testing. Nonetheless, it is crucial to acknowledge that empirical models have limitations and may not capture all aspects of cement-based composite behavior. Furthermore, with the increasing utilization of various cementitious and other materials in concrete, empirical models face added complexity [7–9].

To address these challenges, the integration of machine learning techniques has emerged as a promising avenue [10, 11]. Machine learning offers a data-driven approach that uncovers complex relationships between input features and concrete performance. By leveraging large datasets, machine learning models can predict durability properties while considering the influence of various pertinent factors. This enables the development of highly accurate and scalable predictive models, capable of capturing the intricate effects of different mix components and compositions on concrete durability.

This review aims to provide a comprehensive overview of the current landscape of machine learning applications in the field of concrete durability assessment. Focusing on developments over the past decade, it synthesizes existing research and highlights key advancements in applying machine learning techniques to this field. By elucidating potential benefits, challenges, and future directions of employing machine learning techniques in evaluating concrete durability, this review seeks to catalyze further advancements in the field.

2 Machine learning in concrete durability assessment

2.1 Machine learning basics

Machine learning, a subset of artificial intelligence, focuses on developing algorithms and techniques that allow computers to learn from data and make



predictions or decisions without being explicitly programmed [12, 13]. At its core, machine learning revolves around the idea of building models that can automatically learn and improve from experience. This process typically involves training these models on datasets, where patterns and relationships are extracted to enable the model to make accurate predictions on new, unseen data.

Machine learning is underpinned by fundamental principles encompassing diverse learning paradigms—including supervised, unsupervised, semi-supervised, and reinforcement learning—tailored to distinct scenarios and objectives [12, 14]. Among these, supervised learning stands out, wherein algorithms are trained on labeled datasets, each input paired with a corresponding output. This setup enables the algorithm to learn patterns and relationships between input features and target labels, making it suitable for tasks such as classification and regression [15, 16]. Unsupervised learning offers a contrasting approach, operating on unlabeled datasets to uncover hidden structures, patterns, or relationships within the data. Without explicit guidance, unsupervised learning algorithms autonomously identify clusters of similar data-points or reduce the dimensionality of complex datasets. Clustering algorithms group data-points based on inherent similarities, while dimensionality reduction techniques simplify data representations. Unsupervised learning is valuable for tasks such as customer segmentation, anomaly detection, and exploratory data analysis, where the underlying structure of the data is unknown [17].

Semi-supervised learning amalgamates elements of both supervised and unsupervised learning, leveraging a blend of labeled and unlabeled data during model training. This hybrid approach proves advantageous when labeled data is scarce or costly to obtain. By harnessing additional unlabeled examples, semi-supervised learning algorithms enhance model performance and generalization [18]. In both supervised and semi-supervised learning, two primary interpretations are commonly applied: (i) learning the optimal predictor based on the available data distribution, and (ii) estimating the coefficients of a known structural relationship while leveraging the underlying structure. Reinforcement learning, though less commonly applied, represents an increasingly prominent paradigm. It furnishes a distinct framework for training agents to engage with environments and optimize

cumulative rewards. Through iterative experimentation, reinforcement learning agents refine optimal strategies, guided by feedback in the form of rewards or penalties based on their actions [19, 20].

These foundational principles constitute the backbone of machine learning, yielding a versatile toolkit for tackling an array of challenges across various domains. In the context of concrete science, supervised learning predominates, presenting opportunities to enhance the efficiency, sustainability, and durability of concrete infrastructure through predictive modeling, optimization, and advanced monitoring techniques. In the subsequent sections, the focus shifts to the application of machine learning, emphasizing its contribution to aiding concrete durability assessment.

2.2 Review of machine learning models

To comprehensively review the literature on the application of machine learning models for predicting values for durability indicators of cementitious materials, a systematic methodology was employed. Initially, databases such as Web of Science, Scopus, and Google Scholar were queried using a combination of keywords including “machine learning”, “durability prediction”, “cementitious materials”, “concrete”, and other specific durability phenomena names. The search was restricted to peer-reviewed articles published between 2013 and 2024 to capture the latest advancements. It is important to note that while the review encompasses literature up to 2024, all relevant articles were collected by the end of March 2024. Titles and abstracts of the retrieved papers were screened for relevance, followed by a full-text review of the selected articles. Inclusion criteria focused on studies that specifically utilize machine learning techniques for durability assessment, excluding those with purely theoretical or non-machine learning approaches. The selected papers were then categorized based on the specific durability properties they addressed—such as alkali-silica reaction, carbonation, chloride-induced degradation, sulfate attack, frost damage, shrinkage, corrosion, and thermal cracking—the type of machine learning models used, and the characteristics of the dataset employed. For a focused and robust evaluation, only durability mechanisms explored in at least ten machine learning-based studies were included. These mechanisms comprised carbonation, chloride-induced degradation, corrosion



of steel reinforcement, frost damage, shrinkage, and sulfate attack, representing the most extensively studied areas, as illustrated in Table 1. Key metrics for model performance, such as R^2 value on the test set, were extracted and analyzed to identify trends, strengths, and gaps in the current research landscape. Among the most frequently addressed features in the models are those related to the concrete mix design and exposure aggressiveness, with varying impact levels (Fig. 1). This systematic approach ensured a thorough and unbiased synthesis of existing knowledge, facilitating a clear understanding of the state-of-the-art and guiding future research directions in the field.

2.2.1 Carbonation

Carbonation is a process by which carbonic acid, formed through the interaction of atmospheric CO_2 and moisture, chemically interacts with alkaline phases in hardened concrete forming carbonate phases. In terms of durability, this process lowers the pH of concrete, which is critical for maintaining the protective passivation layer on the steel reinforcement. The prediction of the carbonation depth of concrete over time allows an estimation of the initiation time for corrosion when the limit state is defined as the depassivation of the reinforcement. Currently, researchers are developing prediction models to estimate concrete carbonation-related test results from the perspective of carbon uptake by concrete structures. This relates to the need to estimate the environmental impact of structures in terms of their global warming potential. For this reason, the prediction of the carbonation depth is not sufficient, and the alkaline reserve of concrete needs to be addressed as well. The present review focuses on the durability aspects of the carbonation of concrete, but comments are largely valuable for CO_2 uptake approaches, as well.

The estimation of natural carbonation during the service life of field concrete is relatively complex due to the influence of several factors. These factors include the mix constituents (e.g., types of cement and supplementary cementitious materials (SCMs), chemical admixtures), the mixture design (e.g., relative contents of binders, water-to-binder ratio (w/b), air content, aggregate gradation), structural design and construction techniques (e.g. concrete cover depth, curing, compaction), environmental exposure

and climatic conditions (e.g., indoor, outdoor sheltered, outdoor unsheltered, temperature, humidity, precipitation) [53]. The prolonged process of natural carbonation imposes substantial costs and further complicates the quantification of carbonation in field concrete. To overcome the complexity induced by time constraints, accelerated carbonation tests have been employed to expedite the investigation of various influential parameters on concrete carbonation. Most machine learning models found in the literature rely on data from these accelerated tests to predict carbonation depth [54–63]. While many studies focus on predicting carbonation depth as the model output, a few (e.g., [64] and [54]) have explored the use of the carbonation coefficient as the output variable.

Table 2 summarizes the research papers that employed different machine learning models to predict carbonation depth and rate of a wide range of concrete technologies. Accordingly, most models for the prediction of accelerated carbonation depth focused on binary blended concrete mixtures incorporating fly ash (FA). While these models have achieved high prediction accuracy, certain limitations highlight the need for further research to develop more generalized models. For instance, FA as supplementary cementitious material demonstrates significantly different carbonation behaviour depending on whether it is siliceous fly ash (class F according to ASTM C618) or high-calcium fly ash (class C according to ASTM C618) [65]. Considering no distinction or clarification on the type(s) of FA used for the training implies the possibility of some bias in the model towards one of the types or a weighted average between both. Another important aspect is the range of CO_2 concentrations in the database. It has been reported that accelerated carbonation at ratios higher than 3–4% diverges very substantially from the natural carbonation of concrete under service (occurring at CO_2 concentrations of 0.03–1%, depending on the type of surrounding environment) [66]. The median of the dataset of 6.5% CO_2 is very much above this threshold, posing difficulties for the application of the model to the prediction of natural carbonation of concrete.

In addition to binary blended concrete mixtures incorporating FA, some studies proposed models to predict the carbonation depth of concrete with other SMCs including ground granulated blast furnace slag (GGBFS), steel slag powder (SSP), metakaolin (MK),



Table 1 Overview of durability indicators predicted by machine learning models

Deterioration mechanism	Commonly predicted indicators	Critical features	Examples of experimental test methods
Carbonation	Carbonation depth, pH reduction	CO ₂ concentration, water-to-cement, reactive CaO, curing	Accelerated carbonation tests (e.g., RILEM CPC-18) [21], Chinese method [22], EN 12390-10 [23], EN 12390-12 [24], EN 13295 [25], ISO/DIS 1920-15 [26], Indian method [27], Nordic method [28], Swiss method [29], British method [30]
Chloride attack	Chloride penetration depth, surface chloride concentration, diffusion coefficient	Chloride surface content, water-to-cement, C ₃ A content, curing	Rapid chloride penetration test (RCPT, ASTM C1202) [31], Chloride migration test (NT Build 492) [32], Accelerated diffusion test (NT Build 443) [33], EN 12390-18 [34], ASTM C1556-11a [35], Spanish method [36]
Sulfate attack	Expansion, mass loss, compressive strength loss	Sulfate concentration, wetting and drying cycles, binder type, water-to-cement	ASTM C 452 (mortars length change) [37], ASTM C1012 (mortars expansion, mass variation) [38], USBR 4908 (concrete expansion, mass variation) [39], GB 749-1965 [40], GB/T 2420-1981 [41], GB/T 749-2001 [42], and GB/T 749-2008 [43], Swiss method [29]
Frost attack	Relative dynamic modulus, mass loss, scaling resistance	Air entrainment, water-to-cement, freeze-thaw cycles	ASTM C666 [44], CDF method [45], CEN/TS 12390-9) [46]
Shrinkage	Drying shrinkage strain, autogenous shrinkage strain	Binder type, moisture content, water-to-cement, binder content	ASTM C157 [47] and EN 12390-16 [48] (length change of concrete specimens)
Corrosion of steel reinforcement	Corrosion potential, corrosion rate, mass loss of reinforcement	Cover depth, water-to-cement, time, crack width	Electrochemical tests (Half-cell potential, ASTM C876 [49], TC 154-EMC_1) [50], Linear polarization resistance (LPR, TC 154-EMC_2) [51], Gravimetric mass loss [52]

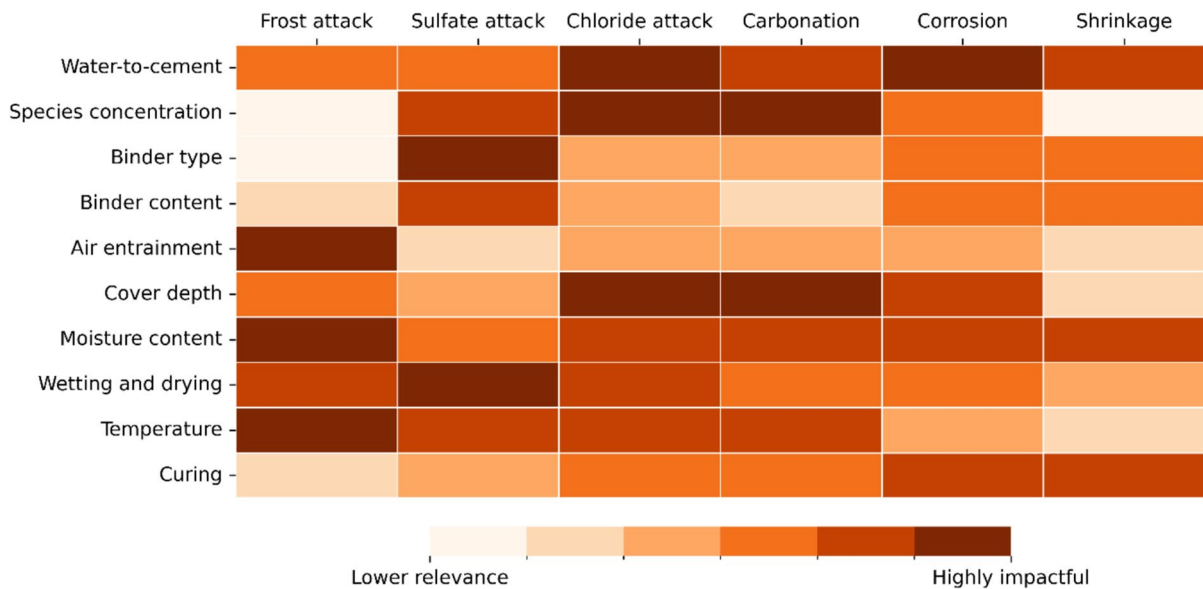


Fig. 1 Comparative impact levels of common features across various deterioration mechanisms

and silica fume (SF). These studies include Wei et al. [59], Duan and Cao [60], Khan and Javed [67] and Taffese et al. [68]. For instance, Taffese et al. [68] used a comprehensive dataset that incorporates six types of cement and three types of SCMs.

In contrast to the majority of studies that focus on accelerated carbonation, Majlesi et al. [69] developed a model to predict the carbonation depth of concrete exposed to long-term (up to 10 years) corrosive environments. They utilized a dataset of 110 instances and incorporated six input features for model development using the ANN algorithm. These features encompassed descriptions of exposure time, concrete quality (capillary absorption, calcium oxide content (CaO)), annual average environmental parameters (temperature and relative humidity), and accumulated precipitation (APP) at the time of carbonation depth measurement. The authors reported a validation accuracy of 0.910. Furthermore, they compared the performance of their model with other machine learning models of DT and MLR on the entire dataset. ANN exhibited a high accuracy with an R^2 value of 0.950, while DT and MLR achieved accuracy of 0.790 and 0.710, respectively. An important limitation of the model is that it was trained with data from concrete made with unblended cement only (CEM I as from EN 197-1), with uncertain applicability to the more

commonly used blended cements nowadays. To address such limitations, Marani et al. [53] developed a probabilistic neural network trained with 2165 data measurements to predict natural carbonation depth of low-carbon concrete incorporating Portland cement and five different types of SCMs. Their model captured the effect of different types of SCMs indicating that FA and limestone and calcined clays accelerate the rate of natural carbonation more significantly compared to ground GGBFS. Additionally, their model successfully learned the effect of regional/geographical climatic exposure on natural carbonation of low-carbon concrete.

Vollpracht et al. [70] used a dataset of 1044 cases, including both concrete and mortar mixes for both natural and accelerated carbonation. Among the binder types, various types of cement and SCMs are considered, with CEM I, CEM II/B-L, CEM II/B-V, CEM II/A, CEM III/B, siliceous FA, GGBFS, and calcined clay being the most present. The XGBoost algorithm was used to derive the permutation feature importance and the SHAP values. This obviously depicted time as the most dominant parameter governing the progression of carbonation depth, followed by CO concentration, concrete strength, clinker content, reactive CaO content, relative humidity, and curing time.

Table 2 Summary of machine learning models to predict accelerated and natural carbonation of concrete

Predicted indicator	Data		Exposure			Model and optimal test performance		Explainability		Publication				
	Concrete type	No of feature	Features category	No of instance	Source	Availability	Condition	Max. period (days)	Algorithm	R ²	Algorithm	Level	Year	References
Car-bonation depth	Natural aggregate, SCMs	25	Mix proportions, engineering properties, environmental conditions	–	Experiments from Finnish DuraInt-project	No	Sheltered Natural and accelerated	2585	BPNN, DT, Bagged DTs	–	–	–	2015	[68]
	Concrete structures	7	Environmental conditions, compressive strength, and cement type	278	Open literature	No	Natural and accelerated	18250 (50 years)	ANN	0.925	–	–	2019	[71]
Car-bonation depth	Normal concrete	9	Mix proportions, test parameters	–	Experiments	No	Accelerated	100	DNN	–	–	–	2020	[54]
Car-bonation depth	RAC with SCMs	17	Mix proportions, engineering properties, environmental conditions	713	Open literature	No	Natural and accelerated	3650	GB	0.971	–	–	2021	[72]

Table 2 (continued)

Predicted indicator	Data	Exposure				Model and optimal test performance		Explainability		Publication				
		Concrete type	No of feature	Features category	No of instance	Source	Availability	Condition	Max. period (days)		Algorithm	R ²	Algorithm	Level
Car-bonation depth	FA blended concrete	5	Binder composition and test parameters	272	Open literature	No	Accelerated	365	ANN and SVM	0.980	Sensitivity analysis	–	2021	[62]
	Recycled aggregate concrete	9	Binder content and test parameters	593	Open literature	No	Accelerated	365	Hybrid ANN-Whale optimization algorithm	0.947	Sensitivity analysis	–	2021	[57]
Car-bonation depth	FA blended concrete	18	Binder composition and test parameters	534	Open literature	No	Natural and accelerated	Not given	ANN, RNN, SVM, tree-based ensembles	0.937	Sensitivity analysis	–	2021	[73]
Car-bonation depth	Concrete with SCMs	29	Mix proportions	8204	Literature	No	Accelerated	Not given	SVR, XGBoost, DNN	–	–	–	2022	[60]
Carbonation rate	Normal concrete	8	Mix proportion and environmental conditions	827	Open literature	No	Accelerated	Not given	Tree-based ensembles	–	–	–	2022	[64]
Car-bonation depth	FA blended concrete	6	Binder amount and test parameters	532	Open literature	Yes	Accelerated	529	Hybrid ANN-SVM	0.995	Sensitivity analysis	–	2022	[55]

Table 2 (continued)

Predicted indicator	Data		Exposure				Model and optimal test performance		Explainability		Publication			
	Concrete type	No of feature	Features category	No of instance	Source	Availability	Condition	Max. period (days)	Algorithm	R ²	Algorithm	Level	Year	References
Car-bonation depth	FA blended concrete	7	Binder amount and environmental condition	688	Open literature	No	Accelerated	365	XGBoost, GB, RF, and SVM	0.977	SHAP	Local	2022	[56]
Car-bonation depth	Concrete containing mineral admixtures	17	Mix proportion and test parameters	1296	Open literature	No	Accelerated	465	ANN and SVM	0.940	Sensitivity analysis	–	2023	[59]
Carbonation rate	Concrete with SCMs	11	Mix proportion ratios	361	Open literature	No	Not Given	Not given	SVM, Decision trees	0.960	SHAP	–	2023	[67]
Car-bonation depth	FA blended concrete	6	Binder composition and test parameters	500	Open literature	No	Accelerated	Not given	Hybrid GWO-LSSVM, WOA-LSSVM, BAS-LSSVM	0.982	Sensitivity analysis	–	2023	[63]
Car-bonation depth	Concrete structures	6	Concrete quality and environmental conditions	Not given	DURA-CON project at 24 urban stations in 10 different countries	No	Natural	2920 (8 years)	ANN	0.976	Sensitivity analysis	–	2023	[69]
Car-bonation depth	FA blended concrete	9 (37)	Mix proportion and test parameters	198	Open literature	No	Accelerated	126	Hybrid ANN	0.995	Feature Importance	–	2024	[58]

Table 2 (continued)

Predicted indicator	Data		Features			Exposure			Model and optimal test performance		Explainability		Publication	
			No of feature	No of instance	Source	Availability	Condition	Max. period (days)						
Car-bonation depth	Concrete type	FA blended concrete	18	830	Open literature	Yes	Accelerated	2070	GPR and ANN	0.906	SHAP	Global	2024	[61]
Car-bonation depth														
	RAC		8	445	Open literature	No	Natural and accelerated	3650 (10 years)	ANN	0.941	Parametric analysis	–	2024	[74]
Car-bonation depth														
	Low-carbon concrete incorporating five types of SCMs		50	2165	Open literature	Yes	Natural	4380 (12 years)	Probabilistic neural network, natural gradient boosting	0.950	Sensitivity analysis	–	2024	[53]



2.2.2 Chloride attack

Chloride-induced deterioration is one of the most significant threats to the durability of RC structures, particularly those exposed to marine environments and deicing salts. In its natural state, concrete provides a highly alkaline environment that fosters the formation of a passive layer on the surface of reinforcement bars, effectively protecting them from corrosion. However, when chloride ions penetrate the concrete and accumulate beyond a critical threshold at the reinforcement level, depassivation occurs, compromising the protective layer and triggering corrosion. This process ultimately undermines the structural integrity, serviceability, and durability of RC structures [75].

In recent years, machine learning has emerged as a transformative tool in modeling and predicting chloride transport behavior. Table 3 provides a summary of machine learning applications over the past decade. Most studies primarily use input features related to mix proportions, with some incorporating environmental conditions and fundamental material properties.

Studies utilizing field datasets predominantly aim to predict surface chloride concentrations in marine environments [76–78], whereas those utilizing laboratory data emphasize modeling chloride ion diffusivity, chloride ion penetration resistance, and chloride profiles. These assessments employ various standardized test methods, including the rapid chloride permeability test [67, 79–83] and the rapid migration test [84–88]. The investigations encompass diverse concrete types, including self-compacting concrete (SCC) [80, 81], high-performance concrete (HPC) [89], and recycled aggregate concrete (RAC) [79].

While most studies concentrate on mix proportions, Tran [85] took a more comprehensive approach by incorporating tricalcium aluminate (C_3A) content of the cement and the specific surface area of fly ash as input features, alongside seven mix-related features, for predicting the chloride diffusion coefficient [90]. Given that C_3A plays a crucial role in chloride binding by reducing ion mobility and delaying chloride transport, its inclusion enhances predictive accuracy. Many laboratory-based studies employing migration tests tend to overlook the chloride binding capacity, particularly when SCMs such as slag and FA are involved. However, a notable limitation in

Tran's study lies in its insufficient distinction between apparent diffusion coefficients derived from two types of accelerated migration tests and those obtained from natural diffusion tests.

Beyond chloride penetration, a select number of studies have embraced a more comprehensive approach by simultaneously predicting multiple durability- or strength-related properties. For instance, Delgado et al. [83] developed models to capture both chloride penetration depth and diffusion coefficients in concrete subjected to drying–wetting cycles. Khan and Javed [67] expanded this scope by predicting chloride permeability, compressive strength, and carbonation resistance. Meanwhile, Wang et al. [82] and Taffese and Espinosa-Leal [91] modeled both chloride penetration rate and compressive strength, albeit through different methodologies—the former relying on passed electric charge, while the latter utilized chloride migration coefficients. These studies underscore the growing shift toward integrated predictive frameworks, paving the way for more robust durability assessments in concrete materials.

Despite regression-based machine learning models being widely utilized in chloride transport studies, classification-based approaches remain underexplored. Typically, chloride transport indexes are used for a qualitative assessment of the concrete performance, yet predictive tools based on classification rather than direct numerical values could offer improved accuracy. For instance, Marks et al. [88] and Taffese and Espinosa-Leal [84] developed machine learning models to classify the chloride resistance levels of concrete. Both studies utilized classification models based on chloride migration coefficients obtained under the Nordic standard NT Build 492 [32]. The former categorized concrete into four resistance classes—Very Good, Good, Acceptable, and Unacceptable—while the latter refined the classification into five levels: Low, Moderate, High, Very High, and Extremely High. These efforts highlight the potential of classification-based machine learning models in providing more interpretable and application-driven assessments of chloride resistance in concrete.

2.2.3 Sulfate attack

Sulfate attack in concrete occurs when sulfate ions from external or internal sources, such as soil,



Table 3 Summary of machine learning models to predict chloride attack-related durability indicators

Predicted indicator	Data		Exposure			Model and optimal test performance		Explainability		Publication				
	Concrete type	No of feature	Features category	No of instance	Source	Availability	Condition	Max. period (days)	Algorithm	R ²	Algorithm	Level	Year	References
Chloride ion diffusivity	Containing mineral and chemical admixtures	4	Mix proportion and exposure time	300	Literature	No	Lab	270	BPNN	Not given	-	-	2013	[89]
	Containing mineral and chemical admixtures	4	Mix proportion and specific surface of fly ash	56	Experiments	Yes	Lab	90	Twenty classifiers based on Bayesian (3), Tree (9) and Rule (8)	N/A	-	-	2015	[88]
Chloride profile	Mortar	4	Presence of reinforcement, exposure time, depth, diffusion dimension	132	Experiments	No	Lab	168	MARS, MGGP, BPNN, LSSVM	0.910	RReliefF	Global	2017	[92]
Chloride ion penetration resistance	SCC containing mineral and chemical admixtures	6	Mix proportion	72	Experiment	Yes	Lab	28	FF-ABC, LR, FF-GA, FF-PSO	0.991	VAF	Global	2019	[80]





Table 3 (continued)

Predicted indicator	Data		Exposure			Model and optimal test performance		Explainability		Publication				
	Concrete type	No of feature	Features category	No of instance	Source	Avail-ability	Condi-tion	Max. period (days)	Algorithm	R ²	Algorithm	Level	Year	Refer-ences
Surface chloride concentration	Contain-ing mineral and chemical admix-tures	13	Mix pro-portion envi-ron-men-tal condi-tions, and expo-sure time	642	Litera-ture	Yes	Field	17757	LR, GPR, SVM, MLP, RF, RF-MLP-SVM	0.830	–	–	2020	[76]
	Chloride ion penetra-tion resist-ance	3	Mix pro-portion, expo-sure condi-tions	360	Experi-ment	Yes	Lab	28	MARS, MPMR	0.935	–	–	2020	[81]
Chloride ion penetra-tion resist-ance	Contain-ing mineral and chemical admix-tures	5	Mix pro-portion, expo-sure condi-tions, Num-ber of Dry-ing—Wetting	243	Experi-ments	No	Lab	98	BPNN	0.955	Not given	Global	2020	[83]

Table 3 (continued)

Predicted indicator	Data	Exposure				Model and optimal test performance		Explainability		Publication				
		No of feature	Features category	No of instance	Source	Availability	Condi-tion	Max. period (days)	Algorithm		R ²	Algorithm	Level	
Chloride ion penetration resistance	RAC containing mineral and chemical admix-tures	8	Mix proportion and aggregate properties	226	Literature	No	Lab	90	GB, GPR, SVM, CART, BPNN, GB	0.958	SRC	Global	2021	[79]
	Surface chloride concentration	13	Mix proportion environmental conditions, and exposure time	642	Literature	Yes	Field	17757	BPNN, DT, GEP	0.880	-	-	2021	[77]



Table 3 (continued)

Predicted indicator	Data	Exposure				Model and optimal test performance		Explainability		Publication				
		No of feature	Features category	No of instance	Source	Availability	Condition	Max. period (days)	Algorithm	R ²	Algorithm	Level	Year	References
Chloride profile	Concrete type	8	Mix proportion and exposure time	120	Literature	No	Lab	270	PSO-BPNN, BPNN	0.967	–	–	2021	[93]
	Basalt–polypropylene fiber reinforced concrete containing coral aggregate, mineral and chemical admixtures	11	Mix proportion and exposure time	204	Literature	Yes	Lab	365	NB, KNN, DT, SVM, RF	N/A	PFI	Global	2022	[84]

Table 3 (continued)

Predicted indicator	Data type	No of feature	Features category	No of instance	Source	Availability	Exposure		Model and optimal test performance	Explainability		Publication	
							Condi-tion	Max. period (days)		Algorithm	Level	Year	Refer-ences
Chloride ion diffusivity	Containing mineral admixtures	9	Mix proportions, C3A and specific surface of fly ash	127	Experiment	Yes	Lab	28	GB, ELM, KNN, Light-GBM, XGBoost, RF, SVM, AdaBoost	SHAP+ICE	Global + Local	2022	[85]
	Containing mineral and chemical admixtures	22	Mix proportion, fresh and hardened concrete properties, and exposure time	843	Literature	Yes	Lab	365	XGBoost, DT, Bagged DTs, RF, AdaBoost, GB	PFI	Global	2022	[86]



Table 3 (continued)

Predicted indicator	Data		Exposure				Model and optimal test performance		Explainability		Publication			
	Concrete type	No of feature	Features category	No of instance	Source	Availability	Condition	Max. period (days)	Algorithm	R ²	Algorithm	Level	Year	References
Chloride profile	Basalt-polypropylene fiber reinforced concrete containing coral aggregate, mineral and chemical admixtures	7	Mix proportion environmental conditions, and exposure time	1650	Literature	No	Field	180	PSO-SVM, SVM, PSO-ANN, MLP	0.994	SHAP	Global	2023	[78]
	Containing mineral and chemical admixtures	11	Mix proportion	323	Literature	No	Lab	Not given	AdaBoost, DT, SVM	0.960	SHAP	Global	2023	[67]

Table 3 (continued)

Predicted indicator	Data		Exposure			Model and optimal test performance		Explainability		Publication				
	Concrete type	No of feature	Features category	No of instance	Source	Availability	Condition	Max. period (days)	Algorithm	R ²	Algorithm	Level	Year	References
Surface chloride concentration	Containing mineral and chemical admixtures	10	Mix proportion, concrete properties, and exposure time	76	Literature	Yes	Lab	28	Bagged DTs, GB, AdaBoost, XGBoost, RF	–	–	–	2023	[91]
	Chloride ion diffusivity	9	Mix proportion and exposure time	204	Literature	Yes	Lab	365	XGBoost	0.870	SHAP + ICE	Global + Local	2024	[87]
Chloride profile	Containing mineral admixtures	8	Mix proportion and exposure time	503	Literature	No	Lab	Not given	RF, GB, DT	0.935	–	–	2024	[94]
Chloride ion penetration resistance	RAC containing mineral admixtures	7	Mix proportion	807	Literature	No	Lab	180	WOA-ANN, GA-ANN, PSO-ANN, BPNN	0.984	SHAP + ICE	Global	2024	[82]



seawater, or industrial effluents, penetrate the cementitious matrix and react with hydration products, leading to chemical transformations that weaken the structure. The primary mechanisms of deterioration include the formation of gypsum and secondary ettringite, which result from the reaction of sulfate ions with calcium aluminate hydrates (C-A-H) and monosulfate phases. These reactions induce expansion, cracking, and loss of cohesion within the material. In aggressive environments, magnesium sulfate can also contribute to deterioration by transforming calcium silicate hydrates (C-S-H) into magnesium silicate hydrates (M-S-H). Additionally, under prolonged exposure and in the presence of carbonates at low temperatures, thaumasite formation may occur, leading to further degradation.

A high concentration of sulfates in the pore solution can also lead to physical attack, this is not a chemical attack but a physical deterioration process instead. Sulfates dissolved in water penetrate unsaturated concrete pores via capillary action (wicking). During drying cycles, water evaporates, concentrating on the sulfate solution until salts crystallize. The crystallization pressure from expanding salts (e.g., mirabilite \rightarrow thenardite) generates internal stresses, leading to fracturing of the concrete matrix. Repeated wetting–drying cycles replenish sulfates and amplify crystallization damage without requiring chemical reactions with cement phases. This mechanism is particularly observed in sulfate-laden environments with fluctuating moisture, such as coastal zones or groundwater-exposed structures. Machine learning models have been applied to predict key deterioration parameters in sulfate-exposed concrete, including strength degradation, mass loss, and expansion. The following subsections provide a detailed review of the algorithms and datasets used for these predictions.

Table 4 summarizes machine learning models used over the past decade to predict durability indicators related to sulfate attack. Most studies focus on strength deterioration, while some model mass loss or expansion. All models use mix proportions and exposure conditions as inputs, with some incorporating clinker composition (notably C_3A content), engineering properties, or sample geometry.

Early models for strength degradation prediction primarily employed ANNs trained on laboratory data. Diab et al. [95] compiled data from 38 studies containing compressive strength, expansion, and weight

loss records. Their ANN model, using cement content, water-to-cement ratio (w/c), C_3A content, sulfate concentration, initial strength, and time, achieved an R^2 of 0.942. Tanyildizi [96] used machine learning models to predict the compressive strength of lightweight cement mortar with SF and FA, with the best ANN model reaching $R^2=0.935$. Chen et al. compared ANN and SVM models for sulfate-exposed mortars using 638 samples from accelerated tests, with ANN performing best.

Recent studies applied ensemble models. Liu et al. [97] used machine learning models to predict sulfate resistance in RAC, with XGBoost achieving $R^2=0.957$, outperforming standalone models (ANN, GPR, SVM, DT). Sun et al. [98] analyzed low-carbon concrete data from 20 references, finding that GWO-optimized SVM performed best ($R^2=0.972$), highlighting water-to-cement ratio (w/b) ratio and wet-dry cycles as key variables.

Few studies addressed mass loss and expansion. Akyuncu et al. [99] used ANN to assess durability in 39 concrete mixtures with Class C and F fly ash, showing improved sulfate resistance regardless of type. Hilloulin et al. [100] compiled 336 expansion curves from literature, interpolated to 5294 data points. XGBoost, optimized via TPE, best predicted expansion curves based on mix proportions, clinker composition, geometry, sulfate solution, and exposure conditions ($R^2=0.933$ on training, 0.788 on test).

In summary, few papers have considered C_3A content, whereas it has been shown experimentally to have a huge influence on the degradation mechanism. Furthermore, in real life, concrete exposed to sulfate-laden environments suffers deterioration due to salt crystallization, which is particularly more pronounced under wet-dry cycles. The inclusion of wet-dry cycles in machine learning studies would help to provide better predictive results for field applications. Notably, no public database exists yet, though explainability tools are emerging to help analyze predictions and enhance model interpretability.

2.2.4 Frost attack

In cold regions, frost damage progresses through cumulative microcracking and surface spalling. When pore saturation in concrete exceeds the saturation threshold, freezing water generates hydrostatic pressure in the pore structure and potential microcrack



Table 4 Summary of machine learning models to predict sulfate attack-related durability indicators

Predicted indicator	Data		Features			Exposure			Model and optimal test performance		Explainability		Publication	
	Concrete type	No of feature	No of instance	Source	Availability	Condition	Max. period (days)	Algo-rithm	R ²	Algo-rithm	Level	Year	References	
Strength degradation	Mortar and concrete	6	2000	Literature	No	Lab	16425	BPNN	0.942	–	–	2014	[95]	
Strength degradation	Light-weight cement mortar	6	288	Literature	No	Lab	365	BPNN, SVM	Not given	–	–	2017	[96]	
Strength degradation	Mortar	10	638	Literature	No	Lab	360	BPNN, SVM	0.999	OAT	Global	2018	[101]	
Mass loss & linear expansion	Concrete containing mineral admixtures	8	180	Literature	No	Lab	365	BPNN	0.980	–	–	2019	[99]	





Table 4 (continued)

Predicted indicator	Data		No of feature	Features category	No of instance	Source	Availability	Exposure		Model and optimal test performance		Explainability		Publication	
	Concrete type							Condition	Max. period (days)	Algo-rithm	R ²	Algo-rithm	Level	Year	References
Strength degradation	RAC		10	Mix proportion, engineering properties, and exposure conditions	143	Literature	No	Lab	365	XGBoost, GB, Ada-Boost, RF, GPR, BPNN, SVM, DT	0.925	TBFI	Global	2022	[97]
	Linear expansion and concrete containing mineral admixtures		21	Mix proportion, clinker composition, sample geometry, sulfate solution and exposure conditions	5294	Literature	No	Lab	1521	XGBoost, DT, LR, LGBM	0.788	SHAP	Global + Local	2023	[100]
Strength degradation	Concrete containing mineral admixtures		9	Mix proportion and exposure conditions	326	Literature	No	Lab	Not given	GWO-SVM, PSO-SVM, SVM	0.972	SHAP	Global	2024	[98]

propagation. Over time, successive freeze–thaw cycles accumulate microcracking, leading to progressive degradation. This deterioration affects mechanical properties and increases permeability, making the concrete more susceptible to environmental damage from harmful substances [102, 103]. Machine learning principles have been explored to identify trends and potentially fast prediction of cement-based composites' performance under such exposures. Table 5 summarizes machine learning models used over the past decade to predict durability indicators related to frost attack. Three main types of applications can be distinguished: direct prediction of durability indicators based on concrete mix proportions, damage degree assessment thanks to the analysis of nondestructive tests and image analysis to qualify air-void system or damage due to freeze–thaw test.

Concerning image analysis, Tian et al. [104] experimentally studied the effect of freeze–thaw action on the internal microstructure of concrete. They used X-ray computed tomography technology (X-ray CT) with deep convolutional neural network for 3D reconstruction of three-phase segmentation. Based on the 3D reconstruction, they studied the effect of freeze–thaw action on the damage evolution in the hydraulic concrete. Additionally, they proposed the formulation for predicting the freeze–thaw life as a function of damage variables. Similarly, Hilloulin et al. [105] proposed a model to segment air-voids in concrete microscopic images to calculate the protected paste volume and showed it is proportional to scaling during freeze–thaw test.

Concerning nondestructive tests results machine learning-mediated analysis, Lian et al. [106] investigated the effect of freeze–thaw cycles on the fracture behavior of concrete using nondestructive testing techniques such as acoustic emission (AE), digital image correlation, and nuclear magnetic resonance techniques. The acoustic emission parameters were used to classify the fracture behavior by employing K-means clustering method. These findings gave valuable insights into the influence of freeze–thaw cycles on the mechanical behavior of concrete. Liao et al. [107] automated the assessment of the freeze–thaw damage in concrete by combining the piezoelectric-based active sensing and deep learning techniques. Two concrete specimens, under no-load and bending states, respectively, were exposed to

freeze–thaw cycles. They acquired the stress wave using PZT transducers which were later converted into time–frequency maps using continuous wavelet transform to obtain the dataset. A novel deep learning model, referred to as the DSC-ACGRU algorithm, was developed for automatic feature extraction. This model combined depth-wise separable convolution, convolutional gated recurrent units, and an attention mechanism. The proposed DSC-ACGRU model exhibited superior efficiency, precision, and accuracy compared to traditional machine learning models (SVM, DT, BPNN) and other deep learning models (CNN, CNN-LSTM).

Several machine learning models have been applied to predict concrete frost resistance based on mix compositions. Liu et al. [108] investigated frost durability in RAC using ANN, GPR, and MARS, with ANN achieving the highest accuracy ($R^2=0.951$). Air entrainment was identified as the dominant factor. Wu et al. [109] developed a hybrid RF-RFE model for predicting high-performance concrete frost resistance, outperforming RF, SVM, PB, and GBDT, with an R^2 of 0.958. Dai et al. [110] evaluated multiple machine learning models on a dataset of 7088 samples, finding nonlinear models more effective. GBDT performed best for relative dynamic elastic modulus ($R^2=0.780$), while CatBoost excelled in mass loss rate prediction ($R^2=0.840$). Atasham ul Haq et al. [111] estimated the deteriorated compressive strength (DCS) after freeze–thaw cycles using ANN, RF, and SVM, all achieving $R^2>0.900$, with ANN performing best ($R^2=0.924$). Sensitivity analysis highlighted the importance of initial concrete strength, lower w/c, and air entrainment. Qiao et al. [112] compared eight models for predicting freeze–thaw damage in dune sand fiber-reinforced concrete (DSFC), where XGBoost emerged as the best ($R^2=0.965$). Esmaeili-Falak et al. [113] optimized SVM with ALO, GWO, and HGSO, with HGSO-SVM achieving the best performance ($R^2=0.997$), revealing cement and sand as key factors. Gao et al. [114] assessed rubberized concrete frost resistance, with XGBoost outperforming DT, ANN, SVM, RF, and stacking methods ($R^2=0.960$). Qin et al. [115] studied freeze–thaw cycles, showing GBM significantly outperformed RF ($R^2=0.990$ vs. 0.930), while GLM and GAM had lower accuracy. The study emphasized the need to

Table 5 Summary of machine learning models to predict frost attack-related durability indicators

Predicted indicator	Data type	Exposure				Model and optimal test performance		Explainability		Publication			
		No of feature	Features category	No of instance	Source	Availability	Condition	Max. period (days)	Algorithm		R ²	Algorithm	Level
Durability factor	RAC	10	Mix proportion and exposure conditions	96	Literature	Yes	Lab	Not given	BPNN, GPR, MARS	0.927	GCV	Global	2021 [108]
	Concrete with FA	12	Mix proportion, test parameters, and exposure conditions	100	Experiments	Yes	Lab	300*	RF, BPNN, SVM, GB	0.958	RF-RFE	Global	2022 [109]
X-ray CT image segmentation	Concrete	N/A	Microscopic images	Not given	Experiments	No	Lab	400*	U-Net	N/A	–	–	2022 [104]
	Concrete	N/A	Microscopic images	Not given	Experiments	No	Lab	56*	Mask RCNN	N/A	–	–	2022 [105]
Classification of AE events	Concrete	N/A	Not given	Not given	Experiments	No	Lab	50*	K-means, KDE	N/A	–	–	2023 [106]
Relative dynamic elastic modulus	Rubberized concrete	7	Mix proportion and exposure conditions	3578	Literature	No	Not given	Not given	RG, BPNN, SVM, XGBoost, Stacked (SVR, XGBoost, LR)	0.960	SHAP+ICE	Global	2023 [114]

Table 5 (continued)

Predicted indicator	Data	Exposure				Model and optimal test performance		Explainability		Publication				
		Concrete type	No of feature	Features category	No of instance	Source	Availability	Condition	Max. period (days)		Algorithm	R ²	Algorithm	Level
Compressive strength loss	Concrete	6	Mix proportion and exposure conditions	155	Literature	Yes	Lab	300*	BPNN, RF, SVM	0.924	SHAP	Global	2023	[111]
	Dune sand and fiber reinforced concrete	8	Mix proportion and exposure conditions	257	Literature	No	Lab	150*	XGBoost, BPNN, SVM, DT, RF, KNN, CatBoost, Light-GBM	0.965	PFI	Global	2023	[112]
Durability factor	RAC	10	Mix proportion and exposure conditions	94	Literature	Yes	Lab	Not given	SVM	0.924	Not given	Global	2023	[113]
Degree of freeze–thaw damage based on time–frequency maps	Concrete	N/A	Continuous wavelet transform (CWT)	1	Experiments	No	Lab	250*	DSC-ACGRU	N/A	–	–	2024	[107]

Table 5 (continued)

Predicted indicator	Data	Exposure				Model and optimal test performance		Explainability		Publication					
		Concrete type	No of feature	Features category	No of instance	Source	Availability	Condition	Max. period (days)		Algorithm	R ²	Algorithm	Level	
Relative dynamic elastic modulus and mass loss rate	Concrete containing mineral and chemical admixtures	Concrete	9	Mix proportion and exposure conditions	7088	Literature	No	Not given	400*	CaBoost, GB, DT, AdaBoost, RF, Light-GBM, MLP, XGBoost, SVM, RBF	0.840	SHAP + ICE	Global + Local	2024	[110]
	Freeze–thaw cycles	Concrete	Not given	Freeze–thaw cycles	Not given	Experiments	No	Field	Not given	GBM, GLM, RF, GAM	0.990	–	–	2024	[115]

*Denotes the number of cycles

improve frost resistance, particularly for regions with more than 200 freeze–thaw cycles.

These findings highlight the increasing use of ensemble learning techniques, particularly XGBoost, GBDT, and RF, in predicting concrete frost resistance, while sensitivity analyses confirm the importance of mix proportions, air entrainment, and w/c ratio in enhancing durability.

2.2.5 Shrinkage

The prediction of autogenous and drying shrinkage properties in cementitious materials is a crucial aspect of concrete technology, as these properties significantly influence the long-term performance and durability of concrete structures. Shrinkage can lead to cracking and reduced structural integrity, making accurate prediction essential for engineers and researchers in the field. While traditional empirical models have provided some insights into shrinkage behavior, they often fall short in capturing the complex interplay of various influencing factors, such as moisture loss, temperature fluctuations, and the inherent material characteristics of the concrete mix.

In recent years, there has been a growing interest in leveraging machine learning techniques to enhance the prediction of shrinkage properties. Few machine learning models have been developed to predict autogenous or drying shrinkage properties of cementitious materials. Table 6 summarizes machine learning models used over the past decade to predict shrinkage.

For drying shrinkage prediction, ANN was deployed by Bal and Buyle-Bodin [116] and Mermedaş and Arbili [117]. The former applied ANN to predict drying shrinkage in normal concrete using a database of 296 specimens, considering 11 parameters related to mix properties, sample geometry, environmental conditions, and 28-day mechanical strength. An R^2 of 0.967 was achieved. On the other hand, Mermedaş and Arbili [117] used experimental data comprising 586 data points from five studies on binary and ternary formulations incorporating silica fume and fly ash. Their results indicated that higher mineral admixture content leads to increased shrinkage strain, with the ANN model accurately predicting experimental values ($R^2=0.954$ on the test set). More recently, ensemble models have been used by Hilloulin and Umunnakwe [118]

and Ocak et al. [119] to predict drying shrinkage in mortar and concrete formulations, incorporating mix compositions, environmental conditions, geometric features, and aggregate properties. Hilloulin and Umunnakwe reported that Extra Trees Regression performed best and provided additional insights through SHAP analysis, while Ocak et al. reported CatBoost was the best model and successfully predicted crack widths due to shrinkage.

Concerning autogenous shrinkage prediction, Liu et al. [120] developed an SVM model for concrete with SF and FA, using eight input parameters. The model outperformed ANN but slightly underestimated shrinkage, showing potential for further improvement. Hilloulin and Tran [121] used ensemble learning on a dataset of 437 studies to predict autogenous shrinkage in cementitious materials with superabsorbent polymers and a broad range of SCMs (calcined clay, slag, FA, SF). XGBoost achieved high accuracy ($R^2=0.954$), and SHAP analysis identified key parameters. A follow-up study [122] showed the optimized model can outperform analytical models (B4, CEB). Similarly, Li et al. [123] used 11 factors to predict autogenous shrinkage in ultra-high-performance concrete (UHPC), with GB providing the best accuracy ($R^2=0.890$). Cement, SF, and water content were most influential, but conflicting results on SF effects suggest variability in its composition.

Finally, Wang et al. [124] predicted nonuniform shrinkage (NUS) in steel–concrete composite slabs using machine learning models. A database of 782 data points from six studies was built, with five input features: relative distance, slab depth, relative humidity, age, and compressive strength. GB emerged as the best model ($R^2=0.927$), and SHAP analysis identified key influencing parameters.

2.2.6 Corrosion of steel reinforcement

Corrosion of reinforcement bars is a major concern in reinforced concrete structures. It typically arises when the protective alkaline environment of the concrete is compromised, allowing aggressive agents to penetrate the concrete and reach the steel reinforcement. Two key parameters characterize the corrosion process in reinforced concrete: the corrosion potential and the corrosion rate. The corrosion potential (electrochemical or half-cell potential) indicates

the likelihood of corrosion occurring, reflecting the thermodynamics of the process. Meanwhile, the corrosion rate measures the speed at which corrosion progresses, representing the kinetics of the process.

As the deterioration advances, a third critical factor comes into play: the development of cracks in the concrete cover. In addition to its chemical protection, the intact concrete cover serves as a physical barrier for the reinforcement bar. However, when cracks form due to the pressure exerted by the expansive corrosion products, the reinforcement becomes significantly more exposed, leading to a rapid acceleration in the corrosion rate.

Zhang et al. [125] used six algorithms, including BR and RF, to predict the integrity of the concrete cover during accelerated corrosion due to chlorides of reinforced concrete with various rubber contents, finding all models except the linear one accurate in estimating cracking due to corrosion.

Nikoo et al. [126] predicted corrosion rate (as obtained from linear polarization resistance) in reinforced concrete using SOFM. It is mentioned that the reinforced concrete was corroded ‘naturally’ but it is unclear if this was a result of carbonation or chloride ingress, implying a big limitation to the utility of the results. Liu et al. [127] evaluated sulfide corrosion rates and initiation times using a hybrid GPR model, which outperformed MLR and RBF models. Sulfide corrosion is comparable to chloride corrosion more than carbonation corrosion, and it implies reinforcement corrosion accelerated by acid attack of cover concrete. Güneyisi et al. [128] used GA and ANN to predict the time from accelerated corrosion initiation to cracking in RC elements, with the ANN model showing higher accuracy. Xu and Jin [129] employed ANN to predict reinforcement corrosion levels, finding the RBF model more accurate than the BP model.

Ji and Ye [130] employed RF, SVM, XGBoost, and ANN to predict corrosion rates in carbonated cementitious mortars, finding SVM to be the most accurate. Salami et al. [131] used LR, ANN, SVM, KNN, and RF to predict corrosion initiation times in steel embedded in SCC exposed to sodium chloride, with RF as the most effective model. Zounemat-Kermani et al. [132] compared neural network-based models (MLP & RBF) and tree-based models (RF, CHAID, & CART) for predicting concrete corrosion in sewers, finding RF superior. Sadowski and Nikoo [133] combined ANN with ICA and GA to predict

Table 6 Summary of machine learning models to predict shrinkage-related durability indicators

Predicted indicator	Data	Exposure					Model and optimal test performance		Explainability		Publication			
		No of feature	Features category	No of instance	Source	Avail-ability	Condi-tion	Max. period (days)	Algorithm	R ²	Algorithm	Level	Year	Refer-ences
Drying shrinkage	Concrete	10	Mix proportion, test parameters and exposure conditions	299	Litera-ture	No	Lab	1200	BPNN	0.967	–	–	2013	[116]
	Concrete with SF and FA	8	Mix proportion	586	Litera-ture	No	Lab	400	BPNN	0.990	–	–	2015	[117]
Autogenous shrinkage	Concrete with SF and FA	8	Mix proportion	518	Litera-ture	No	Lab	15	SVM	0.906	–	–	2016	[120]
Autogenous shrinkage	Mortar and concrete containing mineral and chemical admix-tures	14	Mix proportion and test parameters	1889	Litera-ture	Yes	Lab	28	XGBoost, RF, GB, KNN	0.904	SHAP+ICE	Global + Local	2022	[121]
Autogenous shrinkage	UHPC	11	Mix proportion	159	Litera-ture	No	Lab	7	GB, GPR, SVM, CART, RF, LR, WGBost,BPNN	0.890	SHAP	Global	2023	[123]

Table 6 (continued)

Predicted indicator	Data		Exposure				Model and optimal test performance		Explainability		Publication			
	Concrete type	No of feature	Features category	No of instance	Source	Availability	Condition	Max. period (days)	Algorithm	R ²	Algorithm	Level	Year	References
Drying shrinkage	Mortar and concrete containing mineral admixtures	21	Mix proportion, aggregate properties, test parameters and exposure conditions	3299	Literature	Yes	Lab	1883	ETR, XGBoost, LGBM, RF	0.957	SHAP	Global + Local	2024	[118]
	Drying shrinkage + crack width	5	Mix proportion, mechanical properties and exposure conditions	2640	Literature	No	Lab	60	CatBoost, RF, Bagging Regressor, DT, XGBoost, LGBM, KNN, Adaboost, LR, RG, ElasticNet, Lasso	0.997	–	–	2024	[119]
Non-uniform shrinkage	Steel–concrete composite slabs	5	Engineering properties and exposure conditions	782	Literature	No	Lab	348	GB, KNN, SVM, DT, CART, RF, BPNN, XGBoost	0.927	SHAP	Global + Local	2024	[124]



corrosion current density, with the ICA-ANN model demonstrating enhanced accuracy.

3 Data

3.1 Data source

A detailed examination of the aforementioned machine learning studies reveals some trends regarding the origin of the data. More specifically, as illustrated in Fig. 2, most of the studies (79%) used experimental data from a laboratory environment, while only 14% of the studies reported the use of data from field experiments and the remaining 7% did not mention the origin of the data. The predominance of laboratory studies is unsurprising, as natural degradation mechanisms unfold over extended periods, often spanning decades, making long-term field studies impractical. To circumvent this limitation, researchers frequently employ accelerated testing in controlled environments, enabling them to simulate long-term deterioration within feasible research timelines.

While laboratory experiments offer precise control over influencing factors, they rely on accelerated testing conditions that do not always correlate perfectly to real exposure conditions. Field exposure provides more real results, but the specific exposure conditions are not always relevant for other environments. Moreover, field data frequently originates from structures already exhibiting signs of degradation, as well-performing structures are rarely the subject of durability studies. This introduces an inherent bias: subpar concrete structures in the field tend to be made with mixes below minimum standards, while laboratory studies often use high-quality concrete mixes to ensure broad applicability of results. Consequently, the predictive capabilities and reliability of machine learning models can be inadvertently skewed depending on whether they are trained on field or laboratory data. Furthermore, laboratory tests are performed under controlled conditions that cannot fully replicate the effects of moisture content and transport (e.g., variations in relative humidity, wetting–drying cycles). As a result, the importance of moisture content and transport may be underestimated by models trained solely with lab data. Regardless of whether the studies used experimental data from lab or field

environments, the majority obtained their data from literature sources. For example, of the 79% of studies reporting the use of laboratory data, about half (50%) used data published in the literature and only 28% based their model partially or entirely on their own experiments. Databases consisting of their own results tend to be smaller in size compared to databases constructed from literature. It could be expected that models using field experimental data from literature provide predictions that tend to be more universal but less precise.

Regarding the main temporal trends, the number of machine learning studies focusing on concrete durability has increased over the years, especially since 2019, as shown in Fig. 3. To an extent this is expected as the state-of-the-art machine learning tools have developed significantly in the last 5 years as well. This upsurge is accompanied by an increase in both the number of features and instances in these studies. Initially, most databases contain tens or hundreds of instances. However, most recent studies have leveraged databases with thousands of instances, reflecting a significant expansion in the scope of data utilized.

The number of features incorporated in these studies has varied significantly, ranging from a few as 3 to as many as 37, with a median of 8. Recent research commonly employs between 5 and 15 features. Notably, studies leveraging the largest databases tend to

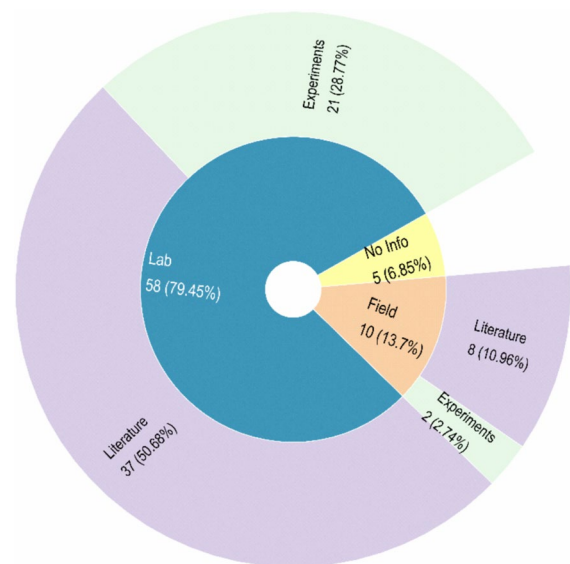


Fig. 2 Dataset sources for the machine learning models



incorporate feature sets exceeding the median, enabling models to more effectively capture and characterize the complex mechanisms governing concrete durability.

In recent years, there has been a noticeable increase in the duration of experiments, measured in the square root of days, considered in machine learning studies focused on concrete durability, as shown in Fig. 4. Conventionally, studies based on laboratory data typically report experiment durations ranging from tens to hundreds of days, often driven by accelerated testing protocols. However, the exposure times reported in more recent research utilizing field data have documented exposure times extending into thousands of days, with the longest reported duration reaching 18,250 days. In contrast to the trend of using more features in larger databases, recent studies with long exposure times do not typically include more than the median number of features. This could be because the existing descriptors are sufficient or because accessing additional descriptive features is

challenging. Moreover, despite being relatively newly published, these documents should not be considered always universally relevant for current construction practices because they are sometimes based on data that is decades old (especially those containing field data). An important aspect to consider is the evolution of binder types, which makes models trained on data that includes only CEM I (or OPC) less up to date.

3.2 Data availability

A significant portion of machine learning studies on concrete durability (68.49%) rely on previously published data, whereas less than one-third (31.51%) generate their own datasets (Fig. 5). Notably, 74% of these studies do not provide open access to their databases. This lack of data transparency is slightly more common in studies using their own data compared to those using curated data. Specifically, only 1 in 5 studies that employ their own experimental data offer

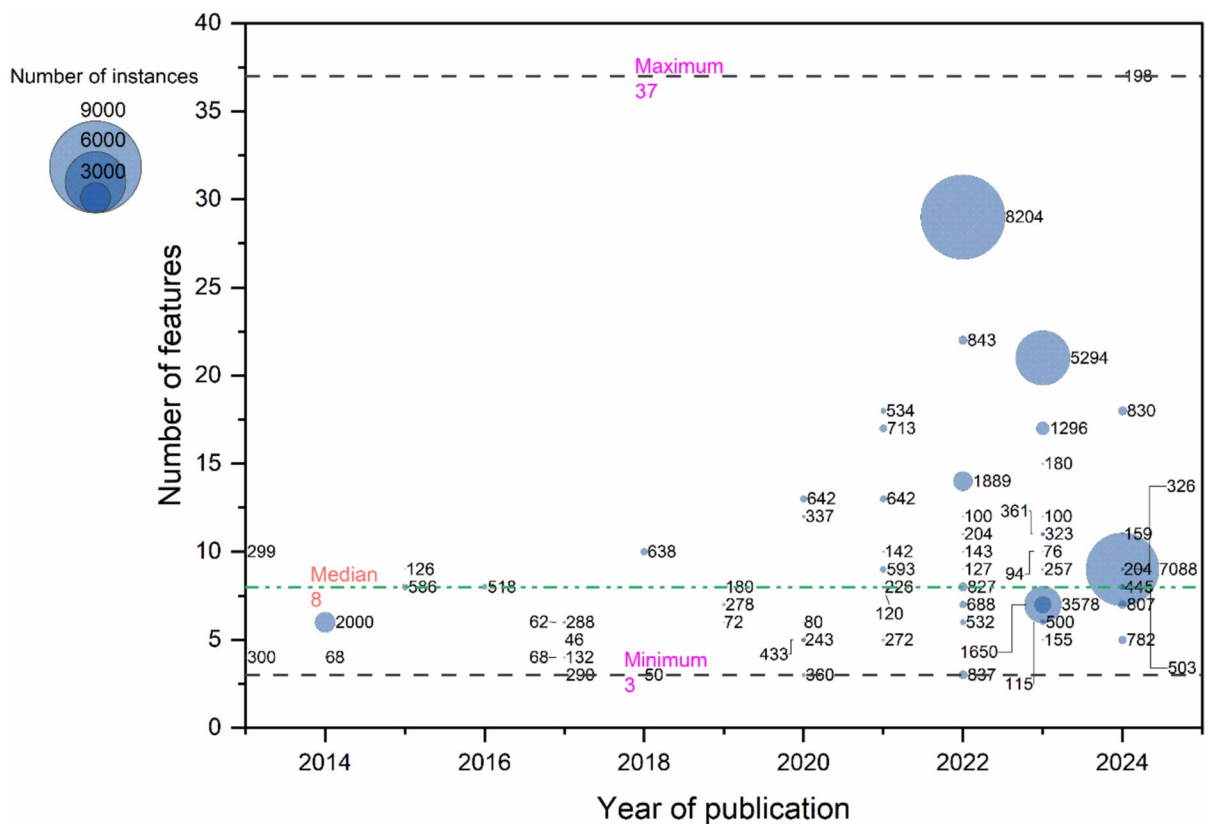


Fig. 3 Number of input features and instances over different years

open access databases, whereas 1 in 3 studies using data from literature. This trend remains surprisingly low even for studies that use data compiled from previous studies. While some data may be sensitive and require confidentiality, it is noteworthy that privately funded research on concrete durability is uncommon, making the reasons for closed access to these databases unclear. However, maintaining closed access to data could potentially mitigate the positive publication bias that is quite prevalent in the field of concrete durability research.

4 Modeling approaches

4.1 Feature types

The first step in the modeling phase involves selecting different features that can be used by the models to describe the durability phenomenon. In machine learning studies focused on the durability

of cementitious materials, these feature types can be categorized into five groups: mixture proportions, engineering properties, exposure conditions, test parameters, and chemical compositions, as illustrated in Fig. 6. It is clear that the majority of the studies primarily consider mix proportions, i.e., mass fractions of constituents, exposure conditions such as temperature and external solution concentration, and test parameters such as concrete age at the start of the test or the test duration. Fewer studies have considered engineering properties, such as specimen size and geometry, or the chemical composition of constituents such as cement. However, a notable shift has emerged in recent years, with increasing emphasis on the inclusion of chemical composition in predictive models. Research has demonstrated that models incorporating binder chemistry significantly outperform those relying solely on cement type, offering deeper insights into material behavior [134]. Despite this advancement, a substantial gap remains in leveraging constituent chemical composition for specific

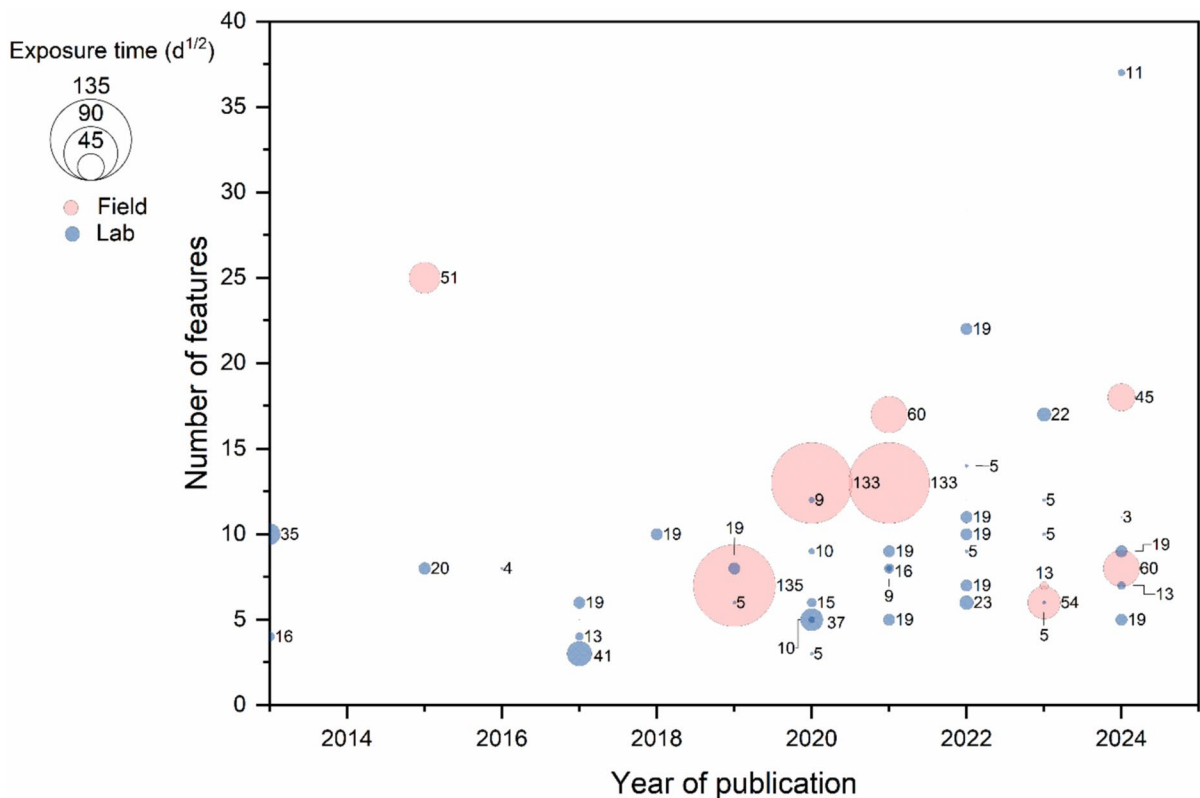


Fig. 4 Exposure time in days for studies using lab and field data over different years



durability challenges such as carbonation, chloride ingress, sulfate attack, corrosion damage, and shrinkage. Addressing this gap presents a crucial opportunity to enhance the predictive accuracy and reliability of durability models.

4.2 Modeling algorithms

As discussed in preceding sections, machine learning studies on concrete durability have employed a variety of models, which can be classically categorized as standalone, ensemble, and hybrid. Standalone models operate independently, making predictions based on a single algorithm. Ensemble models combine multiple standalone models to improve prediction accuracy by leveraging the strengths of each model and mitigating individual weaknesses. Hybrid models integrate different types of algorithms or techniques, such as combining machine learning with statistical methods, to enhance model performance and provide more comprehensive insights into the problem under investigation. Most models used in these studies (148 out of 259, or 57%) fall into the standalone category. Approximately one-third of the models (78 out of 259, or 30%) are ensemble models, and the remainder are classified as hybrid models (33 out of 259, or 13%). A notable trend is the increasing use

of ensemble models over time, particularly after 2020, as depicted in Fig. 7. This shift coincides with the advent of explainability tools, such as the SHAP library, which has enhanced the transparency and understanding of model predictions. It is worth noting that the number of models in 2024 appears to be lower compared to 2023. This is because the present review only includes studies collected by the end of March 2024. It is anticipated that the number of models for 2024 will surpass those from previous years once the entire year's data is accounted for.

Figure 8 provides a breakdown of standalone algorithms utilized in concrete durability research. Neural networks and deep learning methods dominate, appearing 56 times (38%). Kernel methods and probabilistic models are also widely used, with 45 instances (30%). Tree-based methods are used in 21 cases (15%), and regression methods appear 10 times (7%). Other techniques, including instance-based learning, evolutionary algorithms, spline-based methods, density estimation, and clustering, are used less frequently. This diverse array of algorithms highlights the researchers' efforts to explore various approaches to tackle concrete durability issues, with 90% of the standalone algorithms falling into four main categories.

Figure 9 provides a comprehensive overview of the diverse range of algorithms utilized, including standalone, ensemble learning, and hybrid methods. As the standalone algorithms, BPNN leads with 15% (40 instances) of the total, followed by SVM with 12% (32 instances) and DT with 6% (15 instances). In the ensemble learning methods category, RF is the most commonly used with 24 instances, followed by GB and XGBoost, each with 15 instances. Regarding hybrid models, ANNs are most frequently used in conjunction with other algorithms for optimization, followed by SVM optimized using various algorithms. Despite the rapid evolution of new machine learning and deep learning algorithms, many studies have not yet adopted these state-of-the-art methods.

4.3 Models' performance

Figure 10 presents the accuracy (R^2) on the test set of the best regression models reported in the studies for each degradation mechanism. Most of these best R^2 values, ranging from 0.88 to almost 1, are exceptionally high in studies that consider both field and

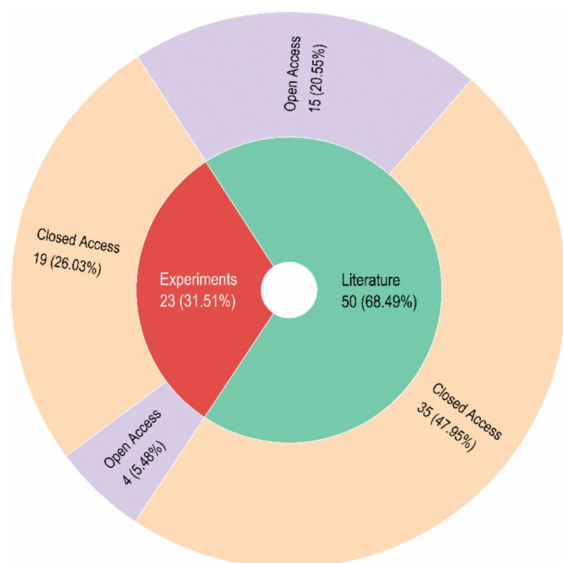


Fig. 5 Publication of data sourced from literature and experiments

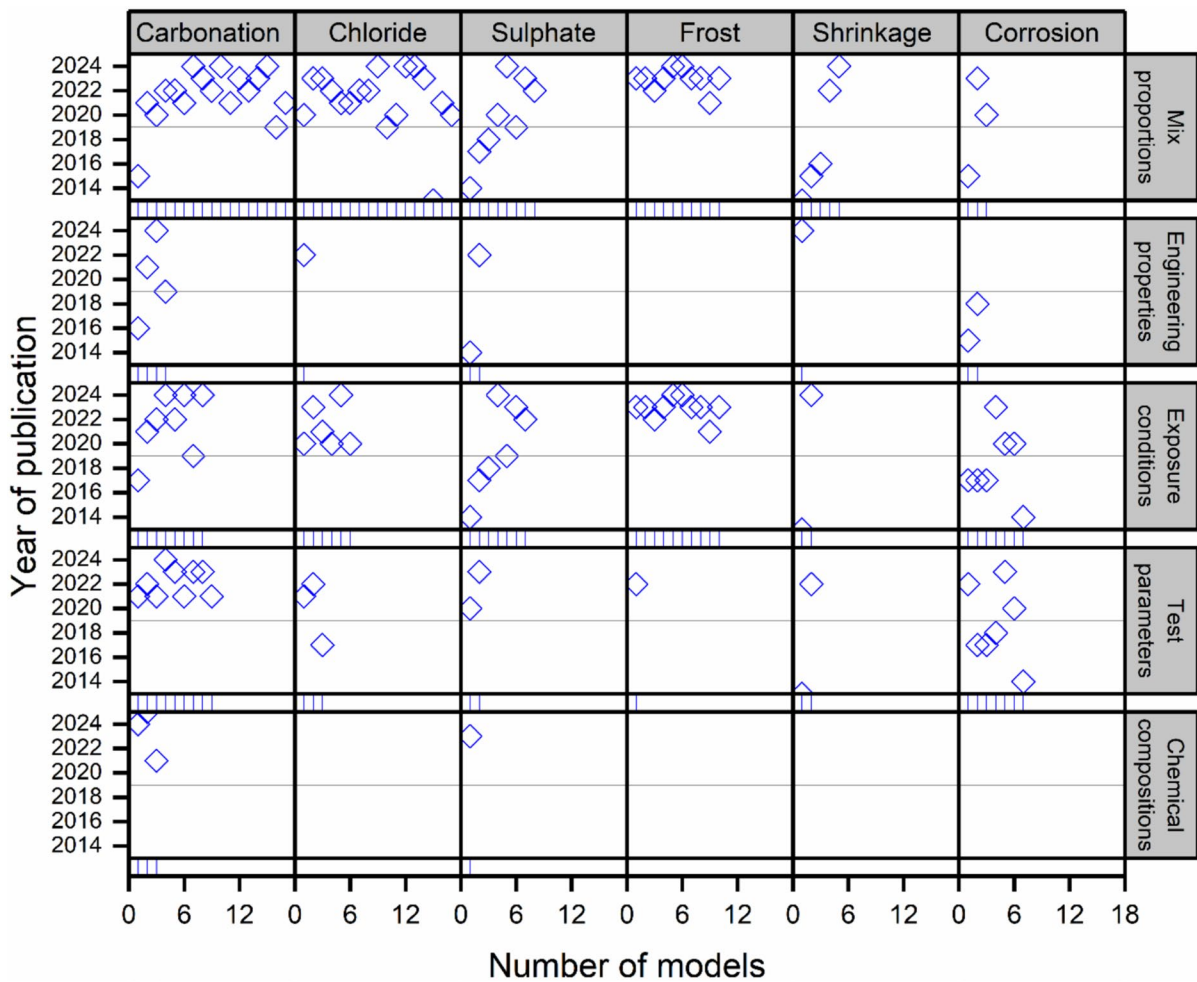


Fig. 6 Categories of input features utilized for each machine learning model under the six degradation mechanisms

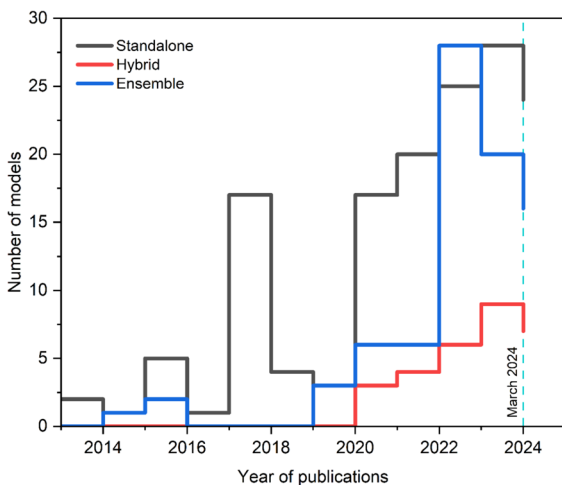


Fig. 7 Evolution of model categories



laboratory data. However, these impressive accuracies sometimes seem too good to be true. This skepticism is heightened by the fact that most of the studies reporting top accuracies—highlighted in red—only compared a limited number of models (typically 1 to 3). Such potential discrepancies in reported accuracy might stem from the considerable variation in data preparation methods, training strategies (e.g., splitting on formulations, others on data-points), the performance evaluation (with or without cross-validation), and the size of the database used. Notably, for field experiments, model performance was reported exclusively for chloride attack and carbonation, as these were the only degradation phenomena modelled using machine learning techniques.

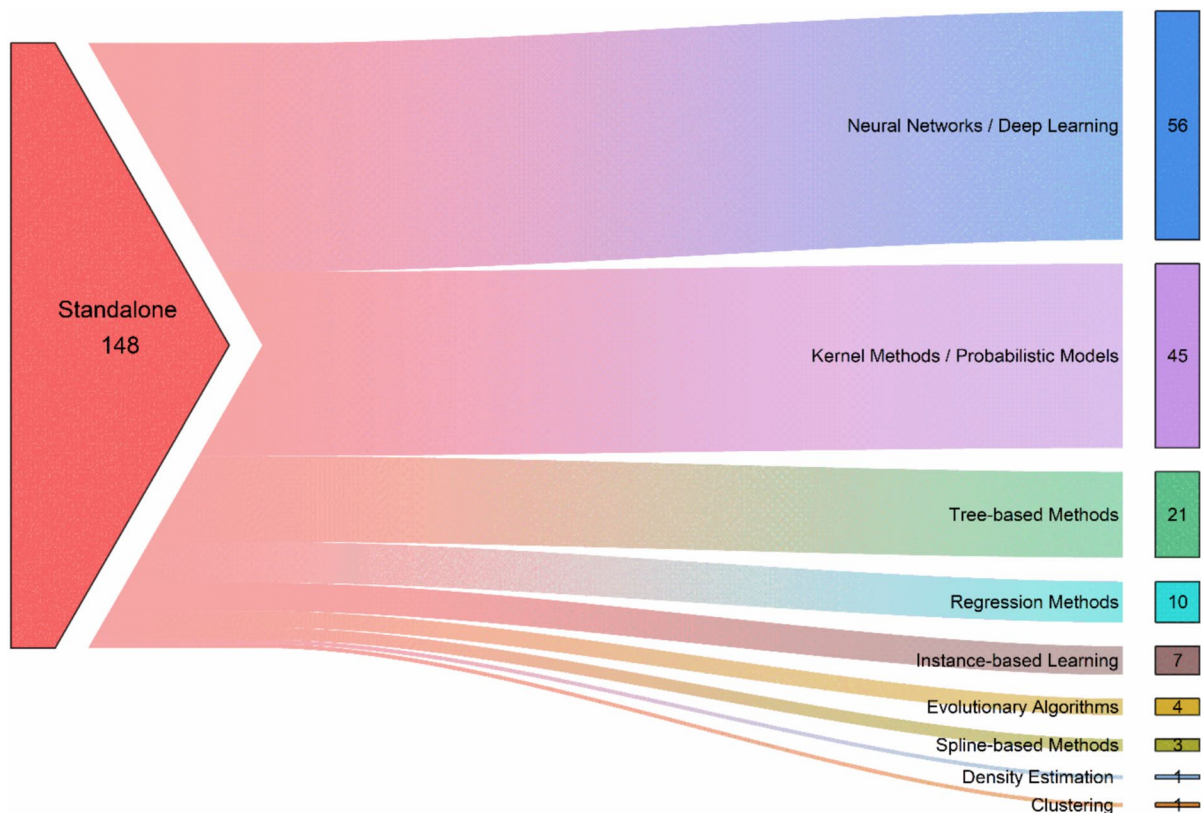


Fig. 8 Categories of standalone algorithms used in the studies

Figure 11 illustrates the types of best models reported across the studies. Ensemble models represent about a third of the best models (36%), while neural networks account for 27%, and hybrid models make up 22%. By comparing this figure with the overall distribution of models used in the studies, it becomes evident that the ensemble models often outperform neural networks, given that their representation among the best models exceeds their share in the total model population. Furthermore, hybrid models also demonstrate significant efficiency, as their share among the best models exceeds their share in the total model population. This indicates a notable trend where hybrid models, though less commonly used, deliver superior performance in predicting concrete degradation mechanisms.

4.4 Models' explainability

While ensuring accuracy in models is crucial for practical applications, model explainability is

equally vital. Model explainability in machine learning can be divided into two primary types: model-agnostic methods and model-specific methods [135–138]. Model-specific methods are designed to align with the unique characteristics of specific machine learning models or groups of models, utilizing their internal structure and properties to create explanations. In contrast, model-agnostic methods are versatile techniques that can be applied to any machine learning model, irrespective of its architecture or underlying algorithm. Figure 12 illustrates the variety and frequency of explainability methods adopted in studies focusing on concrete durability.

Model-agnostic methods are predominant, accounting for 85% of the total (33 instances), compared to 15% for model-specific methods (6 instances). Among model-agnostic techniques, SHAP is the most frequently used, appearing in 25% of the studies. SHAP combined with ICE is also notable, utilized in 15% of the studies. Other model-agnostic

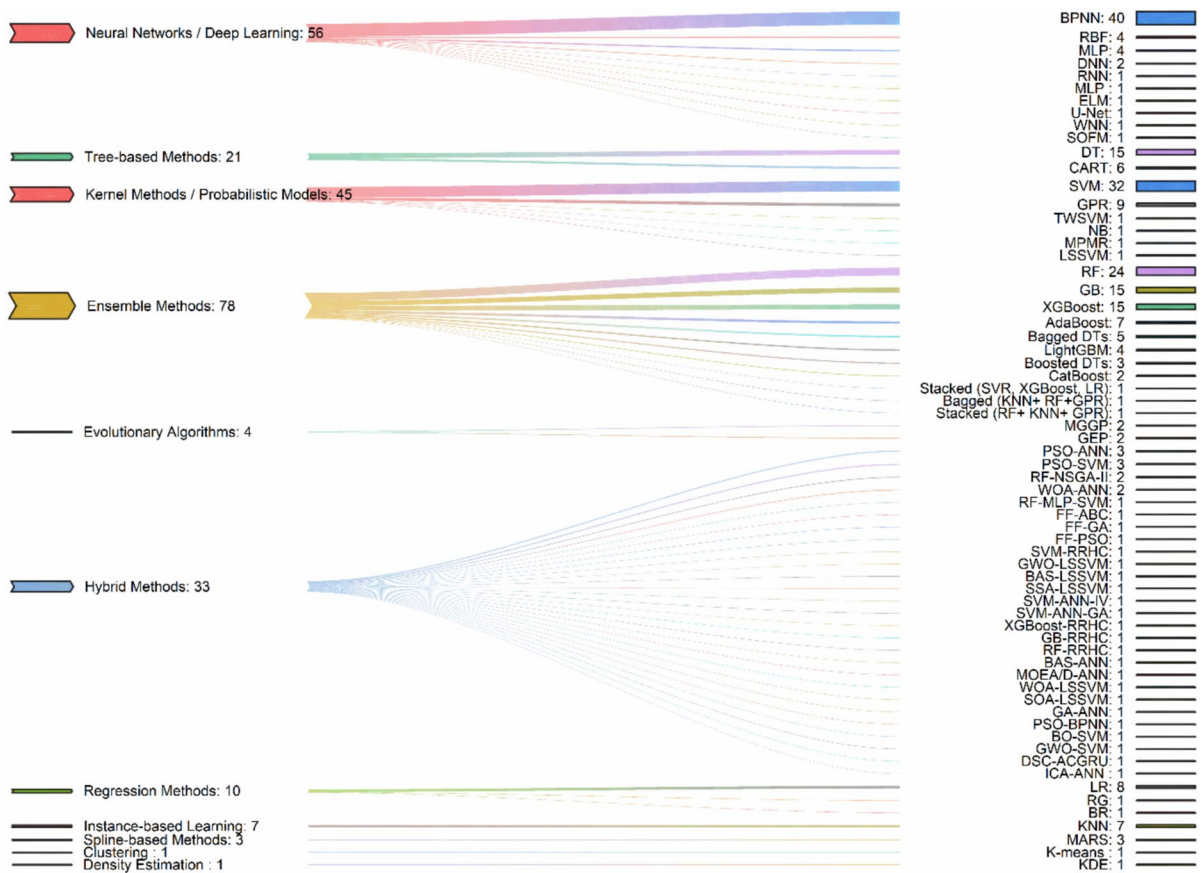


Fig. 9 All types of algorithms used in the studies

methods include PFI (15%), GRA, RReliefF, and p-value analysis (each at 5%), SSIs, GSA, OAT, RF-RFE, and GCV. In contrast, model-specific methods are less diverse and less frequently employed. Among these, SRC is used in 50% of the model-specific studies but appears in only 8% of the total studies, which includes both model-agnostic and model-specific methods. Methods such as MDI, GI, and TBF are each used even less frequently. This preference for model-agnostic methods underscores their flexibility and general applicability in explaining the influence of various features on model predictions, highlighting their importance in advancing the field of concrete durability.

Figure 13 illustrates the extent of model explainability, which can be categorized by global and

combined global–local explainability, applied to various concrete degradation mechanisms. In the earlier years of the examined period, model explainability was not a prominent feature in studies. It was not until 2017 that global model explainability started to gain traction, with a significant increase in studies considering this aspect from 2021 onwards. Unsurprisingly, there are no studies prior to 2022 that incorporate explainability at both the local and global levels. The number of features considered in these models varies significantly, with recent studies tending to incorporate more features, reflecting increased model complexity. Carbonation and chloride studies frequently use global methods with larger feature counts. Studies related to sulfate, frost, and shrinkage employ combined methods, while corrosion studies favor only

Fig. 10 R-square of the best performing models from each study

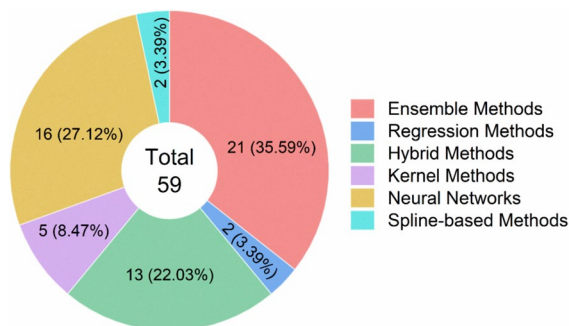
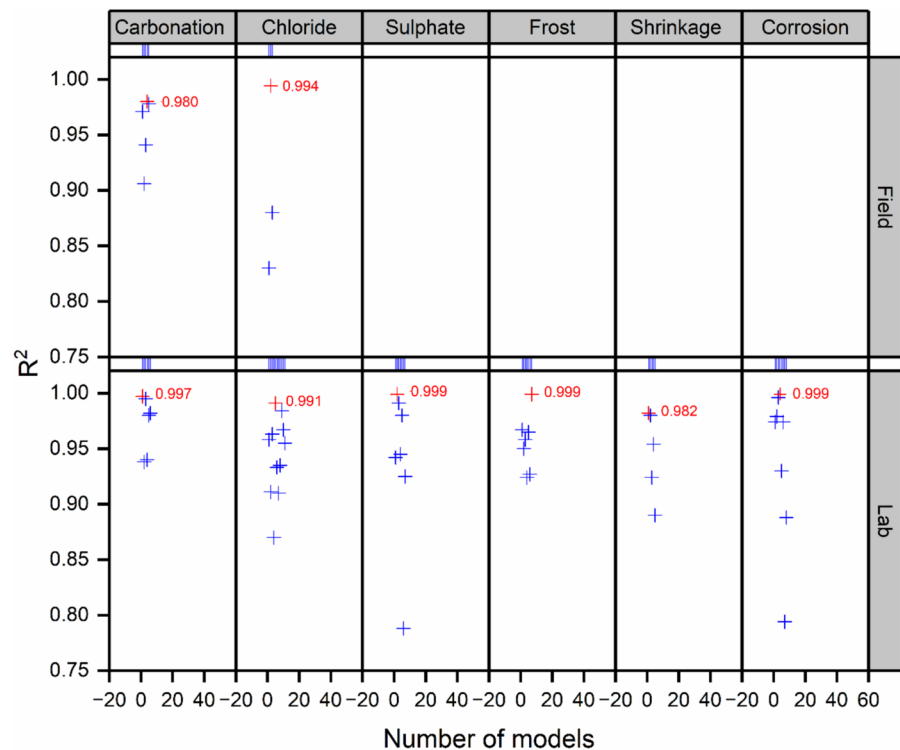


Fig. 11 Percentile share of the category of the algorithm yields best prediction performance

global methods with diverse feature counts. This trend highlights the growing importance of comprehensive model interpretability and the increasing complexity of models in concrete durability research. Given the flexibility and broad applicability of model-agnostic approaches like SHAP, these methods are likely to remain the preferred choice for explaining complex models in the field, enabling deeper insights into degradation mechanisms and model predictions.

5 Discussion

5.1 Benefits and contributions

The utilization of machine learning models to predict the values for durability indicators of cementitious materials offers several significant benefits that revolutionize the field of civil engineering. One of the foremost advantages is their high accuracy in predicting key durability controlling factors such as carbonation, chloride-induced degradation, sulfate attack, frost damage, shrinkage, and corrosion by leveraging vast datasets and advanced algorithms. This level of accuracy surpasses traditional methods, enabling more reliable assessments of concrete structures' longevity and integrity. Moreover, the explainability of these models is a critical feature. The adaptation of explainable machine learning techniques allows engineers to understand the underlying reasons behind the predictions. This transparency is essential for gaining trust in the models and for making informed decisions about concrete durability. Additionally, machine learning models offer a practical alternative

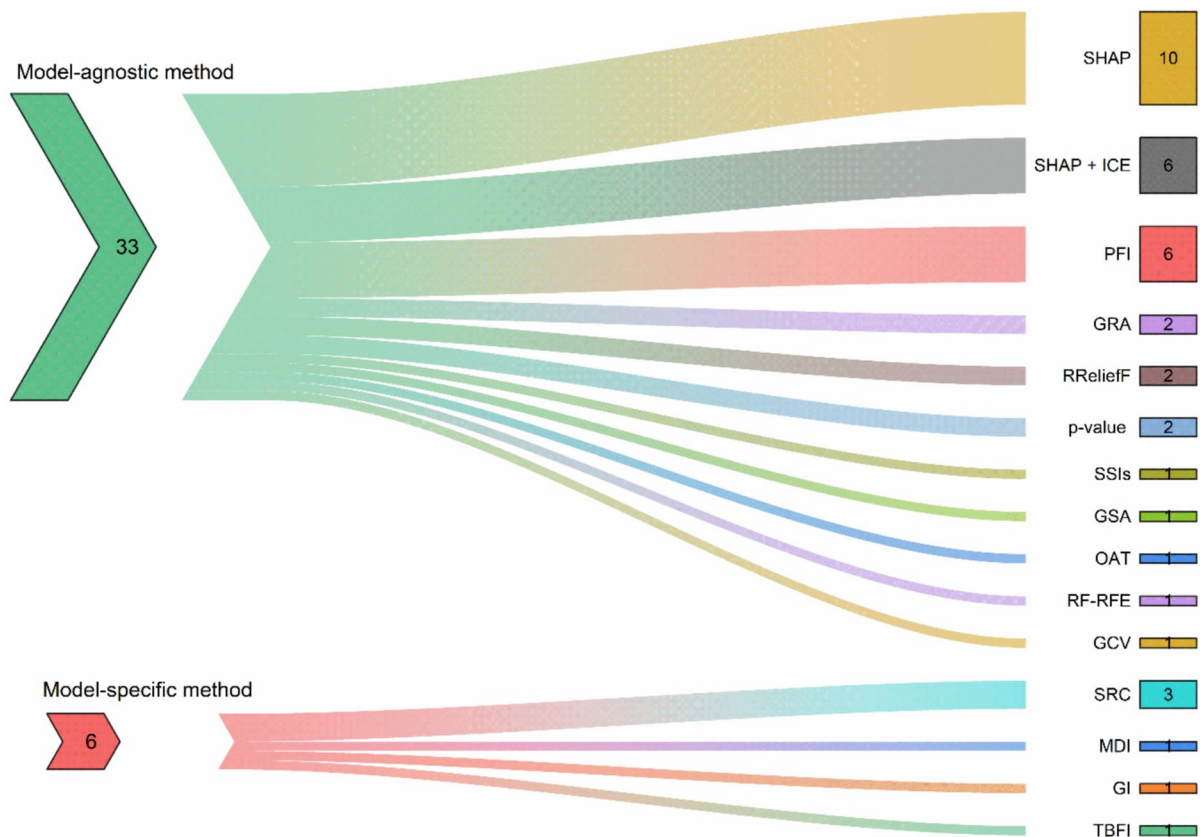


Fig. 12 Methods adopted for model explainability

to time-consuming and resource-intensive laboratory tests. Traditional durability assessments often require extensive sample preparation, long-term exposure studies, and complex testing procedures, all of which consume significant time and resources. In contrast, machine learning models can rapidly analyze large datasets and provide accurate predictions without the need for extensive physical experimentation. This efficiency not only accelerates the assessment process but also reduces costs associated with durability testing. These models are also instrumental in aiding engineers in designing durable concrete structures. By accurately predicting potential degradation mechanisms, engineers can tailor concrete mixtures to mitigate these effects, leading to the development of more resilient infrastructure capable of withstanding environmental stresses.

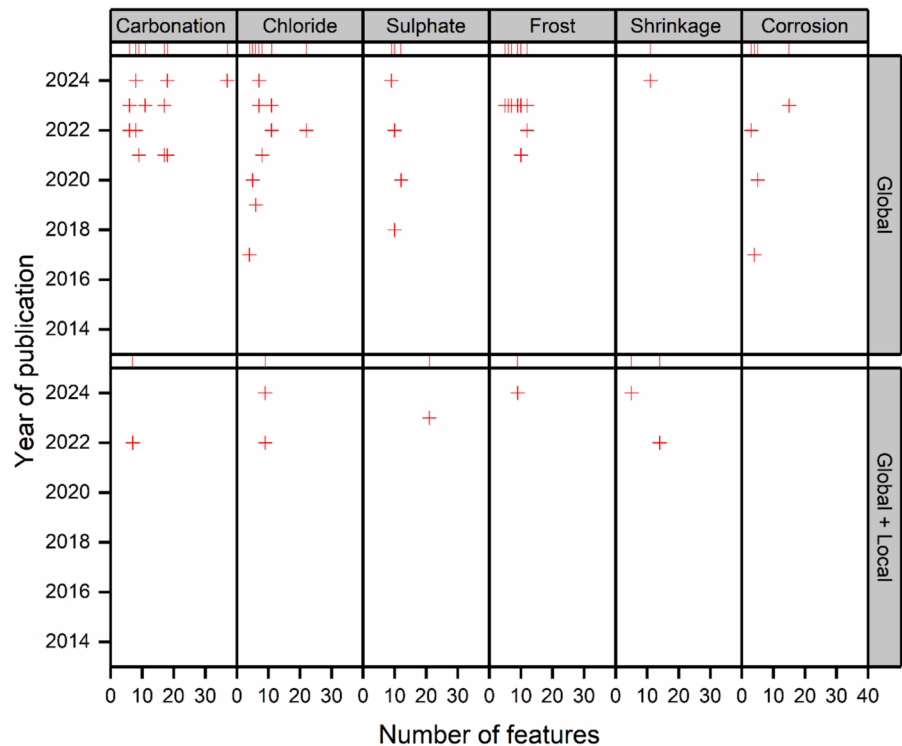
Furthermore, once trained, machine learning models operate faster than conventional numerical models. Numerical simulations, while powerful,

often involve complex computations that can be time-consuming. In contrast, machine learning models, having undergone the initial training phase, can quickly process new data and provide immediate predictions. This speed is particularly advantageous for delivering prompt predictions that expedite the decision-making process in construction projects. Overall, the adoption of machine learning in this context leads to more efficient, cost-effective, and accurate durability assessments, ultimately contributing to the development of infrastructure with extensive service life.

5.2 Current challenges and limitations

Despite the numerous benefits, machine learning models for predicting the values for durability indicators of cementitious materials face several challenges and limitations. One major limitation is that these models often do not account for the various

Fig. 13 Level of model explainability achieved by each study



types of binders used in concrete, potentially limiting their applicability across different formulations. They also tend to consider a limited range of concrete types, which may not fully represent the diversity encountered in real-world applications. Most models are trained with lab databases collecting results from accelerated tests. Such tests offer a good qualitative assessment, but they may fail in predicting the long-term performance of real structures when in service. For instance, a study examining the factors affecting chloride penetration in concrete demonstrated that the relative influence of key features evolves over time [139]. Effects of moisture variations (including dynamic equilibria with the ambient relative humidity, and wetting–drying cycles), frost cycles, chloride deposition rate, CO₂ atmospheric concentration, and thermal cycles may need adaptations for the results from lab-based models. The lack of sufficient field data covering multiple factors is one of the main limitations for developing more comprehensive models. Additionally, the scarcity of substantial open data hampers researchers’ ability to effectively train and validate their models, obstructing replication efforts and hindering collaborative scientific progress. Furthermore, the

generalization capacity of these models is almost always not reported, particularly for concrete with high contents of SCMs, raising concerns about their robustness in diverse scenarios. Another critical challenge is that these models rarely incorporate fundamental physics or chemistry principles, which are essential for a deeper understanding of material behavior. However, there are promising examples of physics-informed machine learning in the field of porous media that could be adapted for concrete technology [140–142]. Addressing these challenges is crucial for advancing the reliability and applicability of machine learning models in predicting the values for durability indicators of cementitious materials.

5.3 Recommendations for future work

To enhance the accuracy and effectiveness of durability experiments as inputs for machine learning models, several best practices should be followed. It is essential to comprehensively report all material and specimen properties, along with detailed descriptions of the experimental conditions. Expanding the availability of field experiment data—particularly those addressing sulfate and frost attack, shrinkage,

and corrosion of reinforcement—would provide invaluable real-world insights that can be used to train, validate, and refine predictive models.

Data reusability should be a primary focus, with researchers encouraged to present readable tables and graphs that are easy to interpret and repurpose for future studies. Beyond individual efforts, collaborative initiatives should focus on developing a comprehensive, standardized data repository, enabling the aggregation of diverse datasets. Such an initiative would significantly advance the field, fostering the development of more robust and generalizable machine learning models capable of capturing the complex interactions influencing concrete durability. Additionally, precise quantification of experimental dispersion is crucial, as it enables the development of models capable of providing uncertainty estimation. This, in turn, enhances the reliability and confidence of predictive models, pushing the boundaries of current research in durability and predictive modeling. Future research should further emphasize the integration of physical and chemical properties of mix constituents, as such an approach enhances predictive accuracy and ensures broader applicability across diverse concrete formulations [134, 143].

Understanding concrete performance is crucial for accurately predicting values of durability indicators and service life of structures. Although most studies assess durability based on individual deterioration mechanisms, real-world conditions often involve combined mechanical and environmental, complicating these evaluations [144, 145]. While sensors play a significant role in monitoring concrete durability environmental conditions [146–149], yet no studies have fully leveraged real-time sensor data. By integrating advanced machine learning techniques with real-time data, researchers can uncover deeper insights into the factors influencing durability. Future research should focus on this innovative approach to enhance the monitoring of concrete performance and strengthen structural resilience.

5.4 Recommendations for machine learning models

When developing machine learning models for predicting values for durability indicators of cementitious materials, several key recommendations should be considered. It is beneficial to use a variety

of feature types to capture the complex interactions influencing material durability. Models should account for the exact amount of SCMs in blended cement to ensure accurate predictions. Proper train-test splits should be performed at the specimen level rather than the data-point level, as multiple data-points can often be derived from a single formulation. Additionally, models should be evaluated using cross-validation to ensure robustness and generalizability. As illustrated in the most recent studies, analyzing results with both global and local model-agnostic interpretation tools can provide deeper insights into model behavior and the factors driving predictions, thereby enhancing the transparency and reliability of the machine learning approach in this domain.

In another perspective, most studies have concentrated on developing machine learning models to predict the outcomes of individual deterioration mechanisms in concrete. However, in real-world scenarios, these degradation mechanisms impact concrete durability both simultaneously and sequentially. It is well-established that synergistic deterioration progresses faster and more severely than any single degradation process [150–152]. Thus, evaluating these combinatory and synergistic effects is crucial for comprehensively addressing concrete durability [153–156]. Current single-task approaches, while effective at predicting complex degradation mechanisms, have significant limitations. Firstly, each task requires separate datasets and models, which is resource intensive. Secondly, these models lack scalability when dealing with degradation influenced by multiple related tasks simultaneously. Thirdly, they do not leverage shared knowledge between related tasks, potentially missing out on performance improvements. A multi-task learning approach is essential for overcoming these limitations. By training a single model to predict multiple degradation processes simultaneously, multi-task learning can enhance predictive capability, especially when degradation mechanisms interact and influence one another, all without significantly increasing model complexity. Since most input features, such as concrete mix composition, are shared across multiple tasks, only a few additional task-specific features are required, making multi-task learning a computationally efficient alternative to multiple independent models. This approach not only uncovers valuable insights but also aids researchers in developing concrete that better resists deterioration mechanisms.



6 Summary

This review highlights the following key findings in the application of machine learning to concrete durability from 2013 to 2024:

- *Data sources and availability:* A dominant reliance on laboratory data (79%) underscores a gap in real-world applicability, as only 14% of studies incorporate field data, with a notable 74% not offering open access to their datasets. This limitation hampers broader validation and the practical application of findings, emphasizing the need for more accessible and diverse data sources.
- *Feature types:* Recent trends reveal a growing emphasis on chemical compositions in modeling, suggesting a shift towards more holistic and nuanced approaches. The integration of diverse features, including mixture proportions, engineering properties, and exposure conditions, reflects a more comprehensive understanding of concrete durability.
- *Modeling approaches:* The adoption of ensemble models has surged, with 33% of studies utilizing them and a significant increase noted post-2020. This shift towards ensemble and hybrid models indicates a move towards more sophisticated and robust predictive techniques, enhancing model accuracy and reliability.
- *Model performance:* Top-performing models exhibit exceptional accuracy, with R^2 values nearing 1 for various degradation mechanisms. Ensemble models lead the pack in performance, followed by neural networks and hybrid models, underscoring their effectiveness in predicting values for concrete durability indicators.
- *Explainability:* There is a strong emphasis on model explainability, with 85% of studies employing model-agnostic methods like SHAP. This focus has intensified since 2017, particularly from 2021 onwards, highlighting the importance of transparency in machine learning models for concrete durability.
- *Recommendations:* To advance the field, it is crucial to develop new, diverse datasets that encompass both chemical and physical properties of mix ingredients. Enhanced data-sharing practices are also essential. Additionally, adopting multi-task learning approaches could provide deeper insights

by addressing multiple deterioration mechanisms simultaneously, paving the way for more durable and resilient concrete structures.

Funding Open Access funding provided by Aalto University.

Open Access This article is licensed under a Creative Commons Attribution 4.0 International License, which permits use, sharing, adaptation, distribution and reproduction in any medium or format, as long as you give appropriate credit to the original author(s) and the source, provide a link to the Creative Commons licence, and indicate if changes were made. The images or other third party material in this article are included in the article's Creative Commons licence, unless indicated otherwise in a credit line to the material. If material is not included in the article's Creative Commons licence and your intended use is not permitted by statutory regulation or exceeds the permitted use, you will need to obtain permission directly from the copyright holder. To view a copy of this licence, visit <http://creativecommons.org/licenses/by/4.0/>.

References

1. Nolan S, Rossini M, Knight C, Nanni A (2021) New directions for reinforced concrete coastal structures. *J Infrastruct Preserv Resil* 2:1. <https://doi.org/10.1186/s43065-021-00015-4>
2. Rabi M, Shamass R, Cashell KA (2022) Structural performance of stainless steel reinforced concrete members: a review. *Constr Build Mater* 325:126673. <https://doi.org/10.1016/j.conbuildmat.2022.126673>
3. fib (2009) Structural concrete textbook on behaviour, design and performance. fib, Lausanne
4. Neville AM, Brooks JJ (2010) Concrete technology, 2nd edn. Pearson Education Limited, Harlow
5. Li Z (2011) Advanced concrete technology. Wiley, New York
6. ACI Committee 201 (2016) Guide to durable concrete. Farmington Hills, MI
7. Beushausen H, Torrent R, Alexander MG (2019) Performance-based approaches for concrete durability: state of the art and future research needs. *Cem Concr Res* 119:11–20. <https://doi.org/10.1016/j.cemconres.2019.01.003>
8. Jamali A, Angst U, Adey B, Elsener B (2013) Modeling of corrosion-induced concrete cover cracking: a critical analysis. *Constr Build Mater* 42:225–237. <https://doi.org/10.1016/j.conbuildmat.2013.01.019>
9. Alexander M, Beushausen H (2019) Durability, service life prediction, and modelling for reinforced concrete structures—review and critique. *Cem Concr Res* 122:17–29. <https://doi.org/10.1016/j.cemconres.2019.04.018>
10. Li Z, Yoon J, Zhang R et al (2022) Machine learning in concrete science: applications, challenges, and best



- practices. *NPJ Comput Mater* 8:127. <https://doi.org/10.1038/s41524-022-00810-x>
11. Taffese WZ, Sistonen E (2017) Machine learning for durability and service-life assessment of reinforced concrete structures: recent advances and future directions. *Autom Constr* 77:1–14. <https://doi.org/10.1016/j.autcon.2017.01.016>
 12. Alpaydin E (2020) Introduction to machine learning, 2nd edn. MIT press, Cambridge, MA
 13. Witten IH, Frank E, Hall MA (2011) Data mining: practical machine learning tools and techniques. Morgan Kaufmann, Burlington, MA
 14. Ivanovic M, Radovanovic M (2015) Modern machine learning techniques and their applications. Electronics, communications and networks. CRC Press, Boca Raton, pp 833–846
 15. Hastie T, Tibshirani R, Friedman J (2009) The elements of statistical learning: data mining, inference, and prediction, 2nd edn. Springer, New York, NY
 16. Bishop CM (2006) Pattern recognition and machine learning. Springer, Cham
 17. Murphy KP (2012) Machine learning: a probabilistic perspective. MIT Press, Cambridge, MA
 18. Chapelle O, Scholkopf B, Zien A (2006) Semi-supervised learning. MIT Press, London
 19. Sutton RS, Barto AG (2018) Reinforcement learning: an introduction, 2nd edn. MIT Press, Cambridge, MA
 20. Mnih V, Kavukcuoglu K, Silver D et al (2015) Human-level control through deep reinforcement learning. *Nature* 518:529–533. <https://doi.org/10.1038/nature14236>
 21. de Rilem R (1988) CPC-18 measurement of hardened concrete carbonation depth. *Mater Struct* 21:453–455. <https://doi.org/10.1007/BF02472327>
 22. GB/T 50082–2009 (2009) Standard for test methods of long-term performance and durability of ordinary concrete
 23. EN 12390–10:2018 (2018) Testing hardened concrete. Part 10. Determination of the carbonation resistance of concrete at atmospheric levels of carbon dioxide
 24. EN 12390–12:2020 (2020) Testing hardened concrete. Part 12. Determination of the carbonation resistance of concrete. Accelerated carbonation method
 25. EN 13295:2004 (2004) Testing hardened concrete. Determination of the carbonation resistance of concrete. Accelerated carbonation method
 26. ISO/DIS 1920–15 (2015) Testing of concrete—part 12: determination of the carbonation resistance of concrete—accelerated carbonation method
 27. IS 516 (2021) Hardened concrete—methods of test part 2: properties of hardened concrete other than strength. Section 4: determination of the carbonation resistance by accelerated carbonation method
 28. NT Build 357 (1989) Concrete, repairing materials and protective coating: carbonation resistance
 29. SIA 262/1 (2019) Concrete construction—additional specifications
 30. BSI (2013) BSI 1881–210:2013 (2013) Testing hardened concrete. Determination of the potential carbonation resistance of concrete. Accelerated carbonation method
 31. ASTM C1202–19 (2019) Test method for electrical indication of concretes ability to resist chloride ion penetration
 32. NT Build 492 (1999) Concrete, mortar and cement-based repair materials: Chloride migration coefficient from non-steady-state migration experiments
 33. NT Build 443 (2011) Testing hardened concrete—part 18: determination of the chloride migration coefficient
 34. EN 12390–18 (2021) Testing hardened concrete—part 18: determination of the chloride migration coefficient
 35. ASTM C1556–11a (2016) Standard test method for determining the apparent chloride diffusion coefficient of cementitious mixtures by bulk diffusion. West Conshohocken, PA
 36. UNE 83992–2:2012 EX (2012) Durability of concrete. Test methods. Chloride penetration tests on concrete. Part 2: integral accelerated method
 37. ASTM C452–21 (2021) Standard test method for potential expansion of portland-cement mortars exposed to sulfate. West Conshohocken, PA
 38. ASTM C1012/C1012M–18b (2024) Standard test method for length change of hydraulic-cement mortars exposed to a sulfate solution. West Conshohocken, PA
 39. USBR 4908 (1986) Procedure for length change of hardened concrete exposed to alkali sulfates. Washington D.C.
 40. (superseded) GB/T 749–1965 (1965) Sulphate resistance test for cement. Beijing
 41. (superseded) GB/T 2420–1981 (1981) Rapid test for sulphate resistance of cement. Beijing
 42. (superseded) GB/T 749–2001 (2001) Test method for potential expansion of portland cement mortars exposed to sulfate. Beijing
 43. GB/T 749–2008 (2008) Test method for determining capability of resisting sulfate corrod. Beijing
 44. ASTM C666–97. Standard test method for resistance of concrete to rapid freezing and thawing. West Conshohocken, PA
 45. Setzer MJ, Fagerlund G, Janssen DJ (1996) CDF test—test method for the freeze-thaw resistance of concrete—tests with sodium chloride solution (CDF). *Mater Struct* 29:523–528. <https://doi.org/10.1007/BF02485951>
 46. CEN/TS 12390–9 (2016) Testing hardened concrete—part 9: freeze-thaw resistance with de-icing salts. Scaling
 47. ASTM C157–75 (1975) Standard test method for length change of hardened cement mortar and concrete. West Conshohocken, PA
 48. EN 12390–16 (2019) Testing hardened concrete—part 16: determination of the shrinkage of concrete
 49. ASTM C876–22b (2022) Standard test method for corrosion potentials of uncoated reinforcing steel in concrete. West Conshohocken, PA
 50. Elsener B, Andrade C, Gulikers J et al (2003) Half-cell potential measurements—potential mapping on reinforced concrete structures. *Mater Struct* 36:461–471. <https://doi.org/10.1007/BF02481526>
 51. Andrade C, Alonso C (2004) Test methods for on-site corrosion rate measurement of steel reinforcement in concrete by means of the polarization resistance method. *Mater Struct* 37:623–643. <https://doi.org/10.1007/BF02483292>



52. ASTM G1-03 (2017)e1 (2017) Standard practice for preparing, cleaning, and evaluating corrosion test specimens. West Conshohocken, PA
53. Marani A, Oyinkanola T, Panesar DK (2024) Probabilistic deep learning prediction of natural carbonation of low-carbon concrete incorporating SCMs. *Cem Concr Compos* 152:105635. <https://doi.org/10.1016/j.cemconcomp.2024.105635>
54. Lee H, Lee H-S, Suraneni P (2020) Evaluation of carbonation progress using AIJ model, FEM analysis, and machine learning algorithms. *Constr Build Mater* 259:119703. <https://doi.org/10.1016/j.conbuildmat.2020.119703>
55. Chen Z, Lin J, Sagoe-Crentsil K, Duan W (2022) Development of hybrid machine learning-based carbonation models with weighting function. *Constr Build Mater* 321:126359. <https://doi.org/10.1016/j.conbuildmat.2022.126359>
56. Tran VQ, Mai HT, To QT, Nguyen MH (2023) Machine learning approach in investigating carbonation depth of concrete containing fly ash. *Struct Concr* 24:2145–2169. <https://doi.org/10.1002/suco.202200269>
57. Liu K, Alam MS, Zhu J et al (2021) Prediction of carbonation depth for recycled aggregate concrete using ANN hybridized with swarm intelligence algorithms. *Constr Build Mater* 301:124382. <https://doi.org/10.1016/j.conbuildmat.2021.124382>
58. Ehsani M, Ostovari M, Mansouri S et al (2024) Machine learning for predicting concrete carbonation depth: a comparative analysis and a novel feature selection. *Constr Build Mater* 417:135331. <https://doi.org/10.1016/j.conbuildmat.2024.135331>
59. Wei Y, Chen P, Cao S et al (2023) Prediction of carbonation depth for concrete containing mineral admixtures based on machine learning. *Arab J Sci Eng* 48:13211–13225. <https://doi.org/10.1007/s13369-023-07645-8>
60. Duan K, Cao S (2022) Data-driven parameter selection and modeling for concrete carbonation. *Materials* 15:3351. <https://doi.org/10.3390/ma15093351>
61. Uwanuakwa ID, Akpınar P (2024) Enhancing the reliability and accuracy of machine learning models for predicting carbonation progress in fly ash-concrete: a multifaceted approach. *Struct Concr* 25:3020–3034. <https://doi.org/10.1002/suco.202300912>
62. Felix EF, Carrazedo R, Possan E (2021) Carbonation model for fly ash concrete based on artificial neural network: development and parametric analysis. *Constr Build Mater* 266:121050. <https://doi.org/10.1016/j.conbuildmat.2020.121050>
63. Zhang K, Zhang K, Bao R, Liu X (2023) A framework for predicting the carbonation depth of concrete incorporating fly ash based on a least squares support vector machine and metaheuristic algorithms. *J Build Eng* 65:105772. <https://doi.org/10.1016/j.job.2022.105772>
64. Londhe S, Kulkarni P, Dixit P et al (2022) Tree based approaches for predicting concrete carbonation coefficient. *Appl Sci* 12:3874. <https://doi.org/10.3390/app12083874>
65. Woyciechowski P, Woliński P, Adamczewski G (2019) Prediction of carbonation progress in concrete containing calcareous fly ash co-binder. *Materials* 12:2665. <https://doi.org/10.3390/ma12172665>
66. von Greve-Dierfeld S, Lothenbach B, Vollpracht A et al (2020) Understanding the carbonation of concrete with supplementary cementitious materials: a critical review by RILEM TC 281-CCC. *Mater Struct* 53:136. <https://doi.org/10.1617/s11527-020-01558-w>
67. Khan M, Javed MF (2023) Towards sustainable construction: machine learning based predictive models for strength and durability characteristics of blended cement concrete. *Mater Today Commun* 37:107428. <https://doi.org/10.1016/j.mtcomm.2023.107428>
68. Taffese WZ, Sistonen E, Puttonen J (2015) CaPrM: carbonation prediction model for reinforced concrete using machine learning methods. *Constr Build Mater* 100:70–82. <https://doi.org/10.1016/j.conbuildmat.2015.09.058>
69. Majlesi A, Khodadadi Koodiani H, Troconis de Rincon O et al (2023) Artificial neural network model to estimate the long-term carbonation depth of concrete exposed to natural environments. *J Build Eng* 74:106545. <https://doi.org/10.1016/j.job.2023.106545>
70. Vollpracht A, Gluth GJG, Rogiers B et al (2024) Report of RILEM TC 281-CCC: insights into factors affecting the carbonation rate of concrete with SCMs revealed from data mining and machine learning approaches. *Mater Struct* 57:206. <https://doi.org/10.1617/s11527-024-02465-0>
71. Felix EF, Possan E, Carrazedo R (2019) Analysis of training parameters in the ANN learning process to mapping the concrete carbonation depth. *J Build Pathol Rehabil* 4:16. <https://doi.org/10.1007/s41024-019-0054-8>
72. Nunez I, Nehdi ML (2021) Machine learning prediction of carbonation depth in recycled aggregate concrete incorporating SCMs. *Constr Build Mater* 287:123027. <https://doi.org/10.1016/j.conbuildmat.2021.123027>
73. Uwanuakwa ID (2021) Deep learning modelling and generalisation of carbonation depth in fly ash blended concrete. *Arab J Sci Eng* 46:4731–4746. <https://doi.org/10.1007/s13369-020-05093-2>
74. Concha NC (2024) A robust carbonation depth model in recycled aggregate concrete (RAC) using neural network. *Expert Syst Appl* 237:121650. <https://doi.org/10.1016/j.eswa.2023.121650>
75. Glass GK (2003) Deterioration of steel reinforced concrete. *Comprehensive structural integrity*. Elsevier, Amsterdam, pp 321–350
76. Cai R, Han T, Liao W et al (2020) Prediction of surface chloride concentration of marine concrete using ensemble machine learning. *Cem Concr Res* 136:106164. <https://doi.org/10.1016/j.cemconres.2020.106164>
77. Ahmad A, Farooq F, Ostrowski KA et al (2021) Application of novel machine learning techniques for predicting the surface chloride concentration in concrete containing waste material. *Materials* 14:2297. <https://doi.org/10.3390/ma14092297>
78. Sun Z, Li Y, Li Y et al (2023) Prediction of chloride ion concentration distribution in basalt-polypropylene fiber reinforced concrete based on optimized machine learning algorithm. *Mater Today Commun* 36:106565. <https://doi.org/10.1016/j.mtcomm.2023.106565>

79. Liu K-H, Zheng J-K, Pacheco-Torgal F, Zhao X-Y (2022) Innovative modeling framework of chloride resistance of recycled aggregate concrete using ensemble-machine-learning methods. *Constr Build Mater* 337:127613. <https://doi.org/10.1016/j.conbuildmat.2022.127613>
80. Najimi M, Ghafoori N, Nikoo M (2019) Modeling chloride penetration in self-consolidating concrete using artificial neural network combined with artificial bee colony algorithm. *J Build Eng* 22:216–226. <https://doi.org/10.1016/j.jobe.2018.12.013>
81. Kumar S, Rai B, Biswas R et al (2020) Prediction of rapid chloride permeability of self-compacting concrete using multivariate adaptive regression spline and minimax probability machine regression. *J Build Eng* 32:101490. <https://doi.org/10.1016/j.jobe.2020.101490>
82. Wang S, Xia P, Gong F et al (2024) Multi objective optimization of recycled aggregate concrete based on explainable machine learning. *J Clean Prod* 445:141045. <https://doi.org/10.1016/j.jclepro.2024.141045>
83. Delgado JMPQ, Silva FAN, Azevedo AC et al (2020) Artificial neural networks to assess the useful life of reinforced concrete elements deteriorated by accelerated chloride tests. *J Build Eng* 31:101445. <https://doi.org/10.1016/j.jobe.2020.101445>
84. Taffese WZ, Espinosa-Leal L (2022) Prediction of chloride resistance level of concrete using machine learning for durability and service life assessment of building structures. *J Build Eng* 60:105146. <https://doi.org/10.1016/j.jobe.2022.105146>
85. Quan Tran V (2022) Machine learning approach for investigating chloride diffusion coefficient of concrete containing supplementary cementitious materials. *Constr Build Mater* 328:127103. <https://doi.org/10.1016/j.conbuildmat.2022.127103>
86. Taffese WZ, Espinosa-Leal L (2022) A machine learning method for predicting the chloride migration coefficient of concrete. *Constr Build Mater* 348:128566. <https://doi.org/10.1016/j.conbuildmat.2022.128566>
87. Taffese WZ, Espinosa-Leal L (2024) Unveiling non-steady chloride migration insights through explainable machine learning. *J Build Eng* 82:108370. <https://doi.org/10.1016/j.jobe.2023.108370>
88. Marks M, Glinicki M, Gibas K (2015) Prediction of the chloride resistance of concrete modified with high calcium fly ash using machine learning. *Materials* 8:8714–8727. <https://doi.org/10.3390/ma8125483>
89. Hodhod OA, Ahmed HI (2013) Developing an artificial neural network model to evaluate chloride diffusivity in high performance concrete. *HBRC J* 9:15–21. <https://doi.org/10.1016/j.hbrj.2013.04.001>
90. Delagrave A, Marchand J, Ollivier J-P et al (1997) Chloride binding capacity of various hydrated cement paste systems. *Adv Cem Based Mater* 6:28–35. [https://doi.org/10.1016/S1065-7355\(97\)90003-1](https://doi.org/10.1016/S1065-7355(97)90003-1)
91. Taffese WZ, Espinosa-Leal L (2023) Multitarget regression models for predicting compressive strength and chloride resistance of concrete. *J Build Eng* 72:106523. <https://doi.org/10.1016/j.jobe.2023.106523>
92. Hoang N-D, Chen C-T, Liao K-W (2017) Prediction of chloride diffusion in cement mortar using multi-gene genetic programming and multivariate adaptive regression splines. *Measurement* 112:141–149. <https://doi.org/10.1016/j.measurement.2017.08.031>
93. Yao L, Ren L, Gong G (2021) Evaluation of chloride diffusion in concrete using PSO-BP and BP neural network. *IOP Conf Ser Earth Environ Sci* 687:012037. <https://doi.org/10.1088/1755-1315/687/1/012037>
94. Wang R, Huo Y, Wang T et al (2024) Machine learning method to explore the correlation between fly ash content and chloride resistance. *Materials* 17:1192. <https://doi.org/10.3390/ma17051192>
95. Diab AM, Elyamany HE, Abd Elmoaty AEM, Shalan AH (2014) Prediction of concrete compressive strength due to long term sulfate attack using neural network. *Alex Eng J* 53:627–642. <https://doi.org/10.1016/j.aej.2014.04.002>
96. Tanyildizi H (2017) Prediction of compressive strength of lightweight mortar exposed to sulfate attack. *Comput Concr* 19:217–226. <https://doi.org/10.12989/cac.2017.19.2.217>
97. Liu K, Dai Z, Zhang R et al (2022) Prediction of the sulfate resistance for recycled aggregate concrete based on ensemble learning algorithms. *Constr Build Mater* 317:125917. <https://doi.org/10.1016/j.conbuildmat.2021.125917>
98. Sun Z, Li Y, Bei Y et al (2024) Compressive strength resistance coefficient of sustainable concrete in sulfate environments: hybrid machine learning model and experimental verification. *Mater Today Commun* 39:108667. <https://doi.org/10.1016/j.mtcomm.2024.108667>
99. Akyuncu V, Uysal M, Tanyildizi H, Sumer M (2019) Modeling the weight and length changes of the concrete exposed to sulfate using artificial neural network. *Rev Constr* 17:337–353. <https://doi.org/10.7764/RDLC.17.3.337>
100. Hilloulou B, Hafidi A, Boudache S, Loukili A (2023) Interpretable ensemble machine learning for the prediction of the expansion of cementitious materials under external sulfate attack. *J Build Eng* 80:107951. <https://doi.org/10.1016/j.jobe.2023.107951>
101. Chen H, Qian C, Liang C, Kang W (2018) An approach for predicting the compressive strength of cement-based materials exposed to sulfate attack. *PLoS ONE* 13:e0191370. <https://doi.org/10.1371/journal.pone.0191370>
102. Wang R, Zhang Q, Li Y (2022) Deterioration of concrete under the coupling effects of freeze–thaw cycles and other actions: a review. *Constr Build Mater* 319:126045. <https://doi.org/10.1016/j.conbuildmat.2021.126045>
103. Guo J, Sun W, Xu Y et al (2022) Damage mechanism and modeling of concrete in freeze–thaw cycles: a review. *Buildings* 12:1317. <https://doi.org/10.3390/buildings12091317>
104. Tian Z, Zhu X, Chen X et al (2022) Microstructure and damage evolution of hydraulic concrete exposed to freeze–thaw cycles. *Constr Build Mater* 346:128466. <https://doi.org/10.1016/j.conbuildmat.2022.128466>
105. Hilloulou B, Bekrine I, Schmitt E, Loukili A (2022) Modular deep learning segmentation algorithm for concrete microscopic images. *Constr Build Mater* 349:128736. <https://doi.org/10.1016/j.conbuildmat.2022.128736>



106. Lian S, Zheng K, Zhao Y et al (2023) Investigation the effect of freeze–thaw cycle on fracture mode classification in concrete based on acoustic emission parameter analysis. *Constr Build Mater* 362:129789. <https://doi.org/10.1016/j.conbuildmat.2022.129789>
107. Liao X, Yan Q, Su L et al (2024) Automatic assessment of freeze-thaw damage in concrete structures using piezoelectric-based active sensing approach and deep learning technique. *Eng Struct* 302:117453. <https://doi.org/10.1016/j.engstruct.2024.117453>
108. Liu K, Zou C, Zhang X, Yan J (2021) Innovative prediction models for the frost durability of recycled aggregate concrete using soft computing methods. *J Build Eng* 34:101822. <https://doi.org/10.1016/j.jobe.2020.101822>
109. Wu X, Zheng S, Feng Z et al (2022) Prediction of the frost resistance of high-performance concrete based on RF-REF: a hybrid prediction approach. *Constr Build Mater* 333:127132. <https://doi.org/10.1016/j.conbuildmat.2022.127132>
110. Dai J, Zhang Z, Yang X et al (2024) Machine learning prediction of concrete frost resistance and optimization design of mix proportions. *J Intell Fuzzy Syst* 48:1–26. <https://doi.org/10.3233/JIFS-236703>
111. Atasham ul haq M, Xu W, Abid M, Gong F (2023) Prediction of progressive frost damage development of concrete using machine-learning algorithms. *Buildings* 13:2451. <https://doi.org/10.3390/buildings13102451>
112. Qiao L, Miao P, Xing G et al (2023) Interpretable machine learning model for predicting freeze-thaw damage of dune sand and fiber reinforced concrete. *Case Stud Constr Mater* 19:e02453. <https://doi.org/10.1016/j.cscm.2023.e02453>
113. Esmaeili-Falak M, Sarkhani Benemaran R (2024) Application of optimization-based regression analysis for evaluation of frost durability of recycled aggregate concrete. *Struct Concr* 25:716–737. <https://doi.org/10.1002/suco.202300566>
114. Gao X, Yang J, Zhu H, Xu J (2023) Estimation of rubberized concrete frost resistance using machine learning techniques. *Constr Build Mater* 371:130778. <https://doi.org/10.1016/j.conbuildmat.2023.130778>
115. Qin Y, Ma H, Zhang L et al (2024) Quantification of the concrete freeze–thaw environment across the Qinghai-Tibet Plateau based on machine learning algorithms. *J Mt Sci* 21:322–334. <https://doi.org/10.1007/s11629-023-8389-7>
116. Bal L, Buyle-Bodin F (2013) Artificial neural network for predicting drying shrinkage of concrete. *Constr Build Mater* 38:248–254. <https://doi.org/10.1016/j.conbuildmat.2012.08.043>
117. Mermerdaş K, Arbili MM (2015) Explicit formulation of drying and autogenous shrinkage of concretes with binary and ternary blends of silica fume and fly ash. *Constr Build Mater* 94:371–379. <https://doi.org/10.1016/j.conbuildmat.2015.07.074>
118. Hilloulin B, Umunnakwe R (2024) Machine learning-aided prediction of shrinkage in modern concrete: focus on mix proportions and SCMs. *J Build Eng* 98:111410. <https://doi.org/10.1016/j.jobe.2024.111410>
119. Ocak A, Bekdaş G, Işıkdag Ü et al (2024) Drying shrinkage and crack width prediction using machine learning in mortars containing different types of industrial by-product fine aggregates. *J Build Eng* 97:110737. <https://doi.org/10.1016/j.jobe.2024.110737>
120. Liu J, Yan K, Zhao X, Hu Y (2016) Prediction of autogenous shrinkage of concretes by support vector machine. *Int J Pavement Res Technol* 9:169–177. <https://doi.org/10.1016/j.ijprt.2016.06.003>
121. Hilloulin B, Tran VQ (2022) Using machine learning techniques for predicting autogenous shrinkage of concrete incorporating superabsorbent polymers and supplementary cementitious materials. *J Build Eng* 49:104086. <https://doi.org/10.1016/j.jobe.2022.104086>
122. Hilloulin B, Tran VQ (2023) Interpretable machine learning model for autogenous shrinkage prediction of low-carbon cementitious materials. *Constr Build Mater* 396:132343. <https://doi.org/10.1016/j.conbuildmat.2023.132343>
123. Li Y, Shen J, Li Y et al (2024) The data-driven research on the autogenous shrinkage of ultra-high performance concrete (UHPC) based on machine learning. *J Build Eng* 82:108373. <https://doi.org/10.1016/j.jobe.2023.108373>
124. Wang S, Liu J, Wang Q et al (2024) Prediction of non-uniform shrinkage of steel-concrete composite slabs based on explainable ensemble machine learning model. *J Build Eng* 88:109002. <https://doi.org/10.1016/j.jobe.2024.109002>
125. Zhang J, Zhang M, Dong B, Ma H (2022) Quantitative evaluation of steel corrosion induced deterioration in rubber concrete by integrating ultrasonic testing, machine learning and mesoscale simulation. *Cem Concr Compos* 128:104426. <https://doi.org/10.1016/j.cemconcomp.2022.104426>
126. Nikoo M, Sadowski Ł, Nikoo M (2017) Prediction of the corrosion current density in reinforced concrete using a self-organizing feature map. *Coatings* 7:160. <https://doi.org/10.3390/coatings7100160>
127. Liu Y, Song Y, Keller J et al (2017) Prediction of concrete corrosion in sewers with hybrid Gaussian processes regression model. *RSC Adv* 7:30894–30903. <https://doi.org/10.1039/C7RA03959J>
128. Güneyisi EM, Mermerdaş K, Güneyisi E, Gesoğlu M (2015) Numerical modeling of time to corrosion induced cover cracking in reinforced concrete using soft-computing based methods. *Mater Struct* 48:1739–1756. <https://doi.org/10.1617/s11527-014-0269-8>
129. Xu Y, Jin R (2018) Measurement of reinforcement corrosion in concrete adopting ultrasonic tests and artificial neural network. *Constr Build Mater* 177:125–133. <https://doi.org/10.1016/j.conbuildmat.2018.05.124>
130. Ji H, Ye H (2023) Machine learning prediction of corrosion rate of steel in carbonated cementitious mortars. *Cem Concr Compos* 143:105256. <https://doi.org/10.1016/j.cemconcomp.2023.105256>
131. Salami BA, Rahman SM, Oyehan TA et al (2020) Ensemble machine learning model for corrosion initiation time estimation of embedded steel reinforced self-compacting concrete. *Measurement* 165:108141. <https://doi.org/10.1016/j.measurement.2020.108141>
132. Zounemat-Kermani M, Stephan D, Barjenbruch M, Hinkelmann R (2020) Ensemble data mining modeling



- in corrosion of concrete sewer: a comparative study of network-based (MLPNN & RBFNN) and tree-based (RF, CHAID, & CART) models. *Adv Eng Inform* 43:101030. <https://doi.org/10.1016/j.aei.2019.101030>
133. Sadowski L, Nikoo M (2014) Corrosion current density prediction in reinforced concrete by imperialist competitive algorithm. *Neural Comput Appl* 25:1627–1638. <https://doi.org/10.1007/s00521-014-1645-6>
 134. Taffese WZ, Nunes S (2024) Machine learning-based prediction of SCC mortar properties across various cement types. In: RILEM conference on sustainable materials & structures: meeting the major challenges of the 21st century–SMS 2024. Toulouse
 135. Allgaier J, Mulansky L, Draelos RL, Pryss R (2023) How does the model make predictions? A systematic literature review on the explainability power of machine learning in healthcare. *Artif Intell Med* 143:102616. <https://doi.org/10.1016/j.artmed.2023.102616>
 136. Adadi A, Berrada M (2018) Peeking inside the black-box: a survey on explainable artificial intelligence (XAI). *IEEE Access* 6:52138–52160. <https://doi.org/10.1109/ACCESS.2018.2870052>
 137. Lipton ZC (2018) The mythos of model interpretability. *Queue* 16:31–57. <https://doi.org/10.1145/3236386.3241340>
 138. Barredo Arrieta A, Díaz-Rodríguez N, Del Ser J et al (2020) Explainable artificial intelligence (XAI): concepts, taxonomies, opportunities and challenges toward responsible AI. *Inf Fusion* 58:82–115. <https://doi.org/10.1016/j.inffus.2019.12.012>
 139. Taffese WZ, Sistonen E (2017) Significance of chloride penetration controlling parameters in concrete: ensemble methods. *Constr Build Mater* 139:9–23. <https://doi.org/10.1016/j.conbuildmat.2017.02.014>
 140. Laloy E, Jacques D (2022) Speeding up reactive transport simulations in cement systems by surrogate geochemical modeling: deep neural networks and k-nearest neighbors. *Transp Porous Media* 143:433–462. <https://doi.org/10.1007/s11242-022-01779-3>
 141. Chen Y, Xu Y, Wang L, Li T (2023) Modeling water flow in unsaturated soils through physics-informed neural network with principled loss function. *Comput Geotech* 161:105546. <https://doi.org/10.1016/j.compgeo.2023.105546>
 142. Wang Y-W, Dai Z-X, Wang G-S et al (2024) A hybrid physics-informed data-driven neural network for CO₂ storage in depleted shale reservoirs. *Pet Sci* 21:286–301. <https://doi.org/10.1016/j.petsci.2023.08.032>
 143. Zhang LV, Marani A, Nehdi ML (2022) Chemistry-informed machine learning prediction of compressive strength for alkali-activated materials. *Constr Build Mater* 316:126103. <https://doi.org/10.1016/j.conbuildmat.2021.126103>
 144. Amey SL, Geiker M, Manning DG et al (2000) Service-life prediction—state-of-the-art report. ACI Committee, Montreal
 145. Holst A, Budelmann H, Wichmann H-J (2011) Improved sensor concepts for durability monitoring of reinforced concrete structures. In: Chang F-K (ed) *Proceedings of the 8th International Workshop on Structural Health Monitoring*. Stanford, CA, pp 1472–1479
 146. Shi X (2024) Online monitoring of reinforced concrete corrosion using sensors. *Eco-efficient repair and rehabilitation of concrete infrastructures*. Elsevier, Amsterdam, pp 85–111
 147. Barroca N, Borges LM, Velez FJ et al (2013) Wireless sensor networks for temperature and humidity monitoring within concrete structures. *Constr Build Mater* 40:1156–1166. <https://doi.org/10.1016/j.conbuildmat.2012.11.087>
 148. Taffese WZ, Nigussie E (2020) Autonomous corrosion assessment of reinforced concrete structures: feasibility study. *Sensors* 20:6825. <https://doi.org/10.3390/s20236825>
 149. Costa AA, Quarcioni VA (2024) Durability monitoring of existing reinforced concrete structures: concepts, advancements, and prospects. *Rev IBRACON Estrut Mater* 17:e17614. <https://doi.org/10.1590/s1983-41952024000600014>
 150. Grantham MG (2011) Understanding defects, testing and inspection. In: Grantham MG (ed) *Concrete repair: a practical guide*. CRC Press, London, pp 1–55
 151. Wittmann FH, Zhao T, Jiang F, Wan X (2012) Influence of combined actions on durability and service life of reinforced concrete structures exposed to aggressive environment. *Restor Build Monum* 18:105–112. <https://doi.org/10.1515/rbm-2012-6510>
 152. Costa A, Appleton J (2001) Concrete carbonation and chloride penetration in a marine environment. *Concr Sci Eng* 3:242–249
 153. Yao Y, Wang L, Li J et al (2023) Report of RILEM TC 281-CCC: effect of loading on the carbonation performance of concrete with supplementary cementitious materials—an interlaboratory comparison of different test methods and related observations. *Mater Struct* 56:110. <https://doi.org/10.1617/s11527-023-02190-0>
 154. Yao Y, Wang L, Wittmann FH et al (2017) Test methods to determine durability of concrete under combined environmental actions and mechanical load: final report of RILEM TC 246-TDC. *Mater Struct* 50:123. <https://doi.org/10.1617/s11527-016-0983-5>
 155. Yao Y, Wang L, Li J et al (2023) Recommendation of RILEM TC 281-CCC: test method to determine the effect of uniaxial compression load and uniaxial tension load on concrete carbonation depth. *Mater Struct* 56:121. <https://doi.org/10.1617/s11527-023-02203-y>
 156. Yao Y, Wang L, Wittmann FH et al (2017) Recommendation of RILEM TC 246-TDC: test methods to determine durability of concrete under combined environmental actions and mechanical load. *Mater Struct* 50:155. <https://doi.org/10.1617/s11527-017-1000-3>

Publisher's Note Springer Nature remains neutral with regard to jurisdictional claims in published maps and institutional affiliations.

